

Peculiar electronic states, symmetries and Berry phases in irradiated α - T_3 materials

Andrii Iurov^{1*}, Godfrey Gumbs^{2,3}, and Danhong Huang^{4,1}

¹*Center for High Technology Materials, University of New Mexico,
1313 Goddard SE, Albuquerque, NM, 87106, USA*

²*Department of Physics and Astronomy, Hunter College of the City
University of New York, 695 Park Avenue, New York, NY 10065, USA*

³*Donostia International Physics Center (DIPC),*

P de Manuel Lardizabal, 4, 20018 San Sebastian, Basque Country, Spain

⁴*Air Force Research Laboratory, Space Vehicles Directorate, Kirtland Air Force Base, NM 87117, USA*
(Dated: September 12, 2018)

We have laid out the results of a rigorous theoretical investigation into the response of electron dressed states, i.e., interacting Floquet states arising from the off-resonant coupling of Dirac spin-1 electrons in the α - T_3 model, to external radiation with various polarizations. Specifically, we have examined the role played by the parameter α that is a measure of the coupling strength with the additional atom at the center of the honeycomb graphene lattice and which, when varied, continuously gives a different Berry phase. We have found that the electronic properties of the α - T_3 model (consisting of a flat band and two cones) could be modified depending on the polarization of the imposed irradiation. We have demonstrated that under elliptically-polarized light the low-energy band structure of such lattice directly depends on the valley index τ . We have obtained and analyzed the corresponding wave functions, their symmetries and the corresponding Berry phases, and revealed that such phases could be finite even for a dice lattice, which has not been observed in the absence of the dressing field. This results lead to possible radiation-generated band structure engineering, as well as experimental and technological realization of such optoelectronic devices and photonic crystals.

PACS numbers: 03.65.Vf, 73.90.+f, 73.43.Cd, 42.50.Ct

I. INTRODUCTION

The α - T_3 model is considered to be the most recent and promising member of novel two-dimensional (2D) materials. Their low-energy dispersions are obtained from a pseudospin-1 Dirac-Weyl Hamiltonian^{1,2} and possess a strong similarity with graphene.³⁻⁵ The atomic structure of the α - T_3 model is represented by a honeycomb lattice with an additional site at the center (a hub atom) of each hexagon. The model Hamiltonian depends on a parameter $\alpha = \tan \phi$ which is a measure of the coupling strength with the extra atom which depends on the ratio of the two hopping coefficients for all hub-rim and rim-to-rim sites. Both α and ϕ may be varied continuously and the Berry phase could be expressed in terms of these two parameters and play a crucial role in affecting many of the electronic and many-body properties of such 2D structures.

The most encouraging technological opportunity for α - T_3 is its applicability for tuning the value of the parameter ϕ from 0 to 1. The results for graphene correspond to the $\alpha \rightarrow 0$ case of this model, while $\alpha \rightarrow 1$ corresponds to a class of existing pseudospin-1 materials.^{1,6,7} Such unique tunability together with additional electron state transitions have made studying various properties of α - T_3 materials as one of the most desirable directions in present-day condensed-matter physics, chemistry and technology.

One of the latest advances in laser and microwave technology has resulted in the possibility of the efficient control, as well as tunability of the basic electronic properties, low-energy band structure including the band gap and the corresponding spin- and valley-dependent electronic states by applying external off-resonant periodic fields. States generated in such a way are referred to as *electron (or optical) dressed states* and represent a single quantum object of strongly coupled light and matter. They are also characterized as an electron dressed by the imposed field of various polarizations, just as it is schematically shown in Fig. 1. The effect of such light-matter interaction on key electron properties could vary substantially depending on the type of polarization of the incoming radiation. Most of the crucial properties of such dressed states could be deduced from conventional Floquet theory, which effectively describes an extremely wide range of quantum mechanical systems under external periodic fields.⁸⁻¹¹ Based on these theories, researchers have developed numerous techniques to modify the existing electronic properties of condensed matter materials, which was subsequently referred to as Floquet engineering of various nanostructures¹²⁻¹⁴ and

* E-mail contact: aiurov@unm.edu, theorist.physics@gmail.com

especially for the novel low-dimensional Dirac cone materials.^{15–22} Considerable effort has been given to find a way to generate topological insulator properties in such systems under irradiation^{12,23,24} Optical dressing can also alter the tunneling and conductance²⁵ properties of a topological insulator, leading to tunable spin transport on their surfaces²⁶ with potential applications in spintronics, as well as result in an optically-stimulated Lifshitz transition.²⁷

Another important property of such electronic dressed systems for operating an optoelectronic device is the challenge of confining such electron states in a specific region. This is directly related to the presence or absence of the so-called Klein paradox²⁸ in the considered material. Circularly-polarized radiation is known to open an energy band gap in initially metallic graphene^{15,29} leading to the suppression of electron transmission^{30,31} or electronic trapping³² with a possible experimental realization. For systems with an already existing band gap, such as buckled honeycomb lattices, the modification of such an energy gap depends on its initial value and could be either increased or reduced,¹⁶ which affects all the collective electronic properties in a non-trivial way.³³ In contrast, radiation with a linear polarization does not generate any band gaps, but leads to strong anisotropy in an exposed material.³⁴ For such anisotropic massless fermions, complete head-on transmission is replaced with asymmetric Klein tunneling³⁵ with a crucial advance for electronic technology, specifically - electron confinement in a low-dimensional material. Such Klein tunneling in the presence of a finite $\alpha < 1$ ³⁶ has been shown to be different from both graphene and dice lattices.³⁷

The principal focus of the present work is to develop a formalism for investigating the properties of optical dressed states for the α - T_3 model corresponding to well-known polarizations of incoming radiations, i.e., elliptical (and circular as a special case) and the linear one. Contrary to previously published recent work,² we concentrate on deriving closed-form analytic approximations and the wave vector dependence of the obtained energy dispersions around each valley, determine and analyze the corresponding wave function, their symmetries, and the corresponding Berry phases which are now significantly modified by electron-light coupling.

The Berry phase was proven to be connected with most physical properties of an α - T_3 lattice.³⁸ Its orbital susceptibility undergoes a transition from diamagnetic in graphene to paramagnetic in a dice material.^{10,39}, which was also shown based on a tight-binding model.⁴⁰ The same applies to the magnetotransport of α - T_3 materials,⁴¹ its conductivity displays several peaks, and each of those peaks is split if α is set finite.^{42,43} Consequently, one of our goals here will be to study how the geometric Berry phase of an α - T_3 lattice is modified in the presence of a dressing field.

The rest of this paper is organized in the following way. In Sec. II, we provide a brief description of the crucial electronic properties, the low-energy band structure in the vicinity of the K and K' valleys, as well as the corresponding electronic wave functions, noting all their possible relations with phase $\phi(\alpha)$. Following this, we present our derivation of the off-resonant electron Floquet states for elliptically, circularly and linearly polarized irradiation. Whenever possible, we also find the corresponding eigenstates for such dressed electrons, discuss their structure and symmetry properties. Specifically, we examine in which all our obtained results depend on $\phi(\alpha)$ and how these relations interplay with electron-field coupling. We also point out for which cases the obtained energy bandstructure becomes directly dependent on the valley index τ . We also calculate Berry phases for all obtained previously obtained eigenstates, providing analytical expressions whenever possible, and discuss their features in Sec. III. Our concluding remarks are provided in Sec. IV and finally, we provide detailed derivations of all our crucial results in Appendices A, B and C.

II. ELECTRON DRESSED STATES

In this section, our goal is to obtain the energy dispersions and the wave functions for the quasiparticle dressed states for elliptical, and circular as its limiting case, and linear polarizations. Considering these situations, we are mainly concerned with elucidating the effect of the phase $\phi(\alpha)$ on the quantities under consideration.

To establish notation, we begin with an overview of the low-energy Hamiltonian, its eigenfunctions and energy dispersions for the α - T_3 model. These states are derived from the ϕ -dependent pseudospin-1 Dirac-Weyl Hamiltonian²

$$\mathbb{H}_\tau^\phi(\mathbf{k}) = \hbar v_F \begin{pmatrix} 0 & k_-^\tau \cos \phi & 0 \\ k_+^\tau \cos \phi & 0 & k_-^\tau \sin \phi \\ 0 & k_+^\tau \sin \phi & 0 \end{pmatrix}, \quad (1)$$

where $k_\pm^\tau = \tau k_x \pm i k_y$ with $\tau = \pm$ labeling the valley and v_F denoting the Fermi velocity. Here, $\alpha = \tan \phi$ represents the principal parameter, characterizing the α - T_3 lattice. For $\alpha = 1$ and $\phi = \pi/4$, the situation is equivalent to the Hamiltonian presented in Ref. [1]. The three solutions for the low-energy band structure, $\varepsilon_{\tau,\phi}^{\gamma=\pm 1}(\mathbf{k}) = \pm \gamma \hbar v_F k$ and

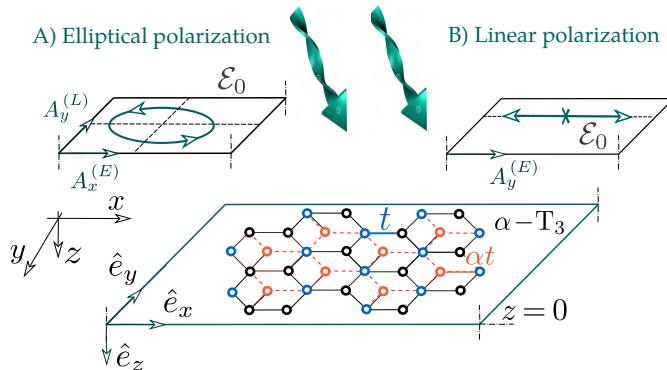


FIG. 1: (Color online) Schematics of an α -T₃ lattice irradiated with A) elliptically- and B) circularly-polarized off-resonance dressing field. In each case, \mathcal{E}_0 is the amplitude of the electric field of the incoming wave.

$\varepsilon_{\tau, \phi}^{\gamma=\pm 1}(\mathbf{k}) = 0$, introduce the valence ($\gamma = -1$), conduction ($\gamma = +1$) and flat bands. All three energy subband energies do not depend on the phase ϕ or α . The corresponding wave functions are

$$\Psi_{\tau, \phi}^{\gamma=\pm 1}(\mathbf{k}) = \frac{1}{\sqrt{2}} \begin{pmatrix} \tau \cos \phi e^{-i\tau\theta_{\mathbf{k}}} \\ \gamma \\ \tau \sin \phi e^{+i\tau\theta_{\mathbf{k}}} \end{pmatrix}, \quad (2)$$

where $\theta_k = \arctan(k_y/k_x)$ is the angle associated with the wave vector \mathbf{k} , $\varepsilon_{\tau, \phi}^{\gamma=\pm 1}(\mathbf{k}) = \gamma \hbar v_F k$ and

$$\Psi_{\tau, \phi}^{\gamma=\pm 1}(\mathbf{k}) = \begin{pmatrix} \sin \phi e^{-i\tau\theta_{\mathbf{k}}} \\ 0 \\ -\cos \phi e^{+i\tau\theta_{\mathbf{k}}} \end{pmatrix}, \quad (3)$$

pertaining to the flat band $\varepsilon_{\tau, \phi}^{\gamma=\pm 1}(\mathbf{k}) = 0$. Unlike the electron dispersions $\varepsilon_{\tau, \phi}^{\gamma=\pm 1}(\mathbf{k})$, most of the crucial properties of the dressed state quasiparticle depend on the phase ϕ or on $\alpha = \tan \phi$.

A. Elliptically-polarized irradiation

The vector potential for elliptically-polarized light depends on the direction of the major axis of the polarization ellipse. Assuming that this direction is collinear with the x -axis, the expression for such a vector potential is¹⁶

$$\mathbf{A}^{(E)}(t) = \begin{Bmatrix} A_x^{(E)}(t) \\ A_y^{(E)}(t) \end{Bmatrix} = \frac{\mathcal{E}_0}{\omega} \begin{Bmatrix} \cos(\omega t) \\ \beta \sin(\omega t) \end{Bmatrix}, \quad (4)$$

where $\beta = \sin \Theta_e$ is the ratio between the axes of the polarization ellipse. Equation (4) represents the most general case of polarization type, $\beta \rightarrow 1$ corresponds to circularly-polarized light with equal but phase-shifted components, while $\beta \rightarrow 0$ describes linearly-polarized irradiation, given by Eq. (23).

It is important to emphasize that for previously studied graphene, the energy dispersions obtained by semi-classical time-dependent representation of the vector potential (4) in Ref. [34] is equivalent to that derived using a quantized field in the limit of large photon occupation numbers.¹⁵

Making use of the canonical substitution $k_{x,y} \rightarrow k_{x,y} - e/\hbar A_{x,y}$, the initial Hamiltonian, given by Eq. (1), is modified as

$$\mathbb{H}_\tau^\phi(\mathbf{k}) \implies \mathcal{H}^{(E)}(\mathbf{k}, t) = \mathbb{H}_\tau^\phi(\mathbf{k}) + \hat{\mathbb{H}}_A^{(E)}(t), \quad (5)$$

where the additional interaction term is

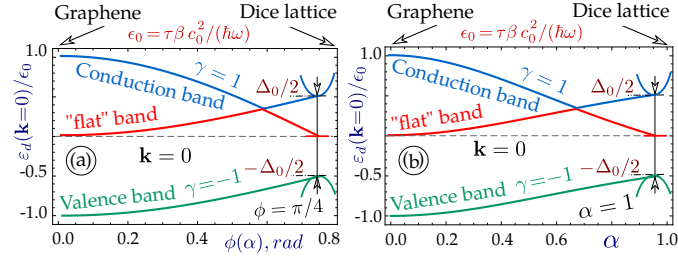


FIG. 2: (Color online) Zero-wavevector (measured at K or K' point depending on the index $\tau = \pm 1$) energies $\varepsilon_d^{(e)}(\mathbf{k} = 0)$ for dressed states in α - T_3 materials under an elliptically-polarized field as a function of parameter $\alpha = \tan \phi$ for panel (a) and α for plot (b). In each panel, the conduction band dispersions are described by a blue curve, the valence band corresponds to a green line, and the flat band to the red ones. The energy separation between the highest (blue) and the lowest (green) dispersion curves defines the *direct band gap* between the valence and conduction bands.

$$\hat{\mathbb{H}}_A^{(E)} = -\tau c_0 \left\{ \begin{bmatrix} 0 & \cos \phi e^{-i\tau \Omega_\beta(t)} & 0 \\ 0 & 0 & \sin \phi e^{-i\tau \Omega_\beta(t)} \\ 0 & 0 & 0 \end{bmatrix} + h.c. \right\}. \quad (6)$$

Here, $+ h.c.$ means adding a Hermitian conjugate matrix to the existing one, $\Omega_\beta(t) = \arctan [\beta \tan(\omega t)]$ is equivalent to (ωt) for circularly-polarized light. The interaction coefficient, equal to $c_0 = v_F e E_0 / \omega$, is equivalent to that for the case of linearly polarized light. E_0 is the amplitude of the imposed electromagnetic wave. Apart from the interaction coefficient $c_0 = v_F e E_0 / \omega$, we will often use a dimensionless coupling constant $\lambda_0 = c_0 / \hbar \omega = v_F e E_0 / (\hbar \omega^2)$. Since all our studies are limited to the case of off-resonant high-frequency irradiation with $\hbar \omega \gg \varepsilon_d(\mathbf{k})$, we can always treat $\lambda_0 \ll a$ an infinitesimal parameter, so that the corresponding series expansions could be carried out.

We would now like to point out that if the initial model Hamiltonian is linear in k , which is the case for nearly all Dirac and gapped Dirac structures, such as gapped or gapless graphene, buckled honeycomb lattices and transition metal dichalcogenides, the resulting Hamiltonian for the dressed states is obtained by adding a single interaction term, independent of the wave vector \mathbf{k} . However, the situation is drastically different for phosphorene with a more complicated anisotropic wave vector dependence in the unperturbed Hamiltonian.¹⁷

In order to solve this eigenvalue problem, we are going to apply *perturbation theory*. Nearly all off-resonant systems, subjected to external periodic fields with $\varepsilon_d(\mathbf{k}) \ll \hbar \omega$, could be effectively described by a perturbation expansion of the interaction Hamiltonian in powers of $1/(\hbar \omega)$. In many cases, this would allow for an approximate solution, while the exact diagonalization of the interaction matrix is not possible,¹⁶ or substantially simplify the existing calculations.¹⁷

The key idea of the perturbation approach is the following. Once the interaction Hamiltonian term $\hat{\mathbb{H}}_A^{(C)}$ is expressed as

$$\hat{\mathbb{H}}_A^{(E)} = \hat{\mathbb{P}}_{\tau, \phi} e^{i\omega t} + \hat{\mathbb{P}}_{\tau, \phi}^\dagger e^{-i\omega t}, \quad (7)$$

where the operator $\hat{\mathbb{P}}_{\tau, \phi}$ and its Hermitian conjugate $\hat{\mathbb{P}}_{\tau, \phi}^\dagger$ are *time-independent*, the effective Hamiltonian representing our dressed states becomes⁸

$$\hat{\mathcal{H}}_{\text{eff}}^{(E)} = \mathbb{H}_\tau^\phi(\mathbf{k}) + \frac{1}{\hbar \omega} \left[\hat{\mathbb{P}}_{\tau, \phi}, \hat{\mathbb{P}}_{\tau, \phi}^\dagger \right] + \frac{1}{2(\hbar \omega)^2} \left\{ \left[\left[\hat{\mathbb{P}}_{\tau, \phi}, \mathbb{H}_\tau^\phi(\mathbf{k}) \right], \hat{\mathbb{P}}_{\tau, \phi}^\dagger \right] + h.c. \right\} + \dots \quad (8)$$

For most of such considerations, it is sufficient to explicitly obtain two terms of such a power series. In our case, the time-independent perturbation operator $\hat{\mathbb{P}}_{\tau, \phi}$ is obtained as

$$\hat{\mathbb{P}}_{\tau, \phi} = -\frac{c_0}{2} \begin{bmatrix} 0 & (\tau - \beta) \cos \phi & 0 \\ (\tau + \beta) \cos \phi & 0 & (\tau - \beta) \sin \phi \\ 0 & (\tau + \beta) \sin \phi & 0 \end{bmatrix}. \quad (9)$$

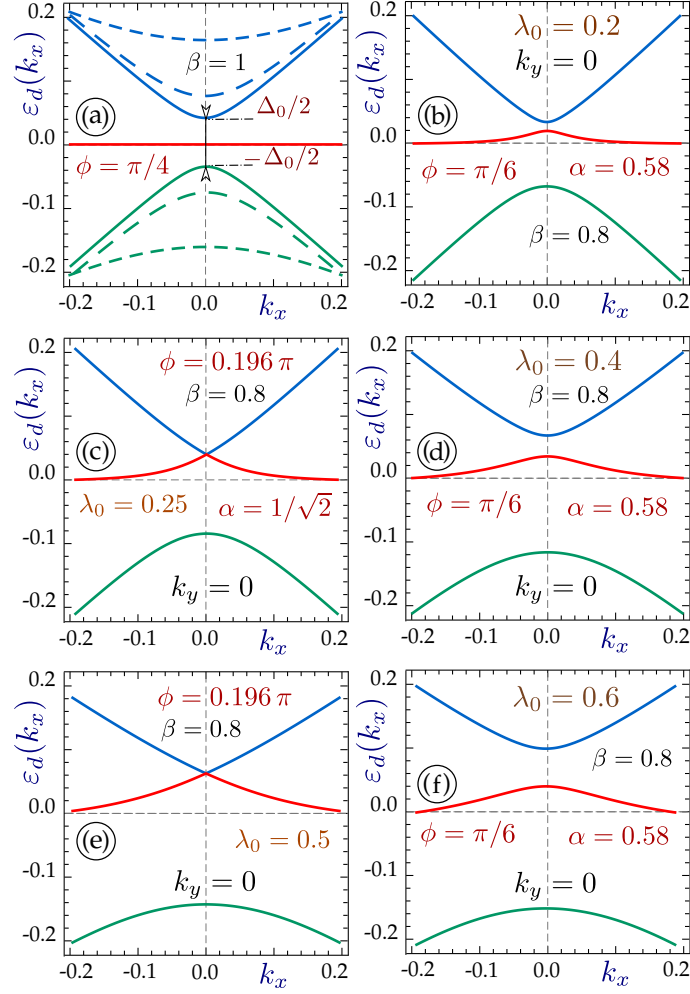


FIG. 3: (Color online) Energy dispersions of a dressed state in an α - T_3 lattice under elliptically polarized off-resonant irradiation with $\beta = 0.8$ as a function of the x -component of the wave vector k_x for $k_y = 0$. All results are obtained in the vicinity of the K valley with $\tau = 1$. Each plot represents the dispersions corresponding to three subbands, i.e., the conduction ($\gamma = 1$, upper blue curve), valence ($\gamma = -1$, lower green line) and the “flat” band (middle red curve). Panel (a) demonstrates the energy dispersions for a dice lattice ($\phi = \pi/4$). All the remaining left plots (c) and (e) correspond to the phase $\phi = 0.196\pi$ or $\alpha = 1/\sqrt{2}$, for which one of the band gaps is zero. All the right panels (b), (d) and (f) are related to $\phi = \pi/6$ and are distinguished by the value of the dimensionless electron-light coupling constant $\lambda_0 = 0.2$ for plot (b), 0.4 for (d) and 0.6 for (f), similar to three different curves for each band in plot (a). Panel (c) corresponds to $\lambda_0 = 0.25$, and plot (e) to 0.5 .

This matrix is real, but clearly not Hermitian, as it always occurs for all types of circularly-polarized irradiation, including the more general case of elliptic polarization with $0 \leq \beta < 1$.

Evaluating the commutation relation in Eq. (8), we arrive at the following expression for the effective perturbation Hamiltonian

$$\hat{\mathcal{H}}_{\text{eff}}^{(E)}(\mathbf{k}, t) = \mathbb{H}_\tau^\phi(\mathbf{k}) - \tau\beta\lambda_0 c_0 \begin{bmatrix} \cos^2 \phi & 0 & 0 \\ 0 & -\cos(2\phi) & 0 \\ 0 & 0 & -\sin^2 \phi \end{bmatrix} - \frac{\tau}{4} \hbar v_F \lambda_0^2 \begin{bmatrix} 0 & h_{12} & 0 \\ h_{12}^* & 0 & h_{23} \\ 0 & h_{23}^* & 0 \end{bmatrix}, \quad (10)$$

where $h_{12}(\beta|\tau, \phi) = \cos \phi [1 + 3 \cos(2\phi)] (\beta^2 k_x - i\tau k_y)$ and $h_{23}(\beta|\tau, \phi) = \sin \phi [1 - 3 \cos(2\phi)] (\beta^2 k_x - i\tau k_y)$.

It is interesting to note that the chirality $\tau k_x \pm i k_y$ of the second perturbation term is the same as that in the unperturbed Hamiltonian $\mathbb{H}_\tau^\phi(\mathbf{k})$ given by Eq. (1).

One needs to pay close attention to the first perturbation term, which is independent of the wave vector \mathbf{k} and determines the position of each band edge at the K point

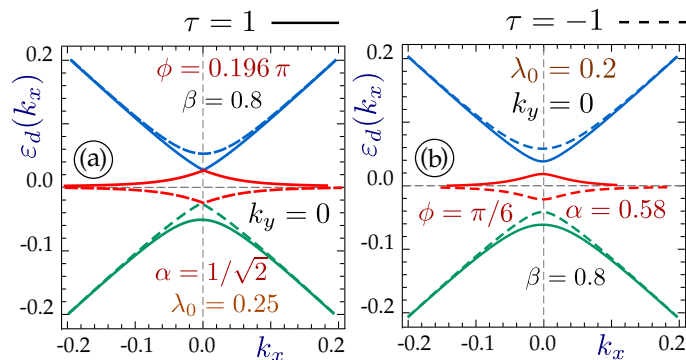


FIG. 4: (Color online) Effect of valley index τ on the energy dispersions of a dressed state in an α - T_3 lattice under elliptically-polarized dressing field. We plot the energy dispersions $\varepsilon_d^{(E)}(\mathbf{k})$ as a function of the x -component of the wave vector k_x for $k_y = 0$. Panel (a) describes the dispersions for $\alpha = 1/\sqrt{2}$ when one of the gaps is closed, while panel (b) shows plots for $\phi = \pi/6$ and $\alpha = 0.586$. In each plot, the solid lines correspond to the K valley or $\tau = +1$, and the dashed ones to the K' with $\tau = -1$ and the dimensionless electron-light coupling constant $\lambda_0 = 0.25$.

$$\varepsilon_d^{(E)}(\mathbf{k} = 0) = \tau\beta \frac{c_0^2}{\hbar\omega} \times \begin{cases} -\cos^2 \phi \\ +\cos(2\phi) \\ +\sin^2 \phi \end{cases} = \tau\beta \lambda_0 c_0 \times \begin{cases} -(1 + \alpha^2)^{-1} \\ (1 - \alpha^2) / (1 + \alpha^2) \\ \alpha^2 / (1 + \alpha^2) \end{cases} \quad (11)$$

as well as the energy gap between the valence and conduction bands

$$\Delta_0(\beta, \phi | \lambda_0) = \frac{\beta}{2} \lambda_0 c_0 \begin{cases} \cos(2\phi) + \cos^2 \phi & \text{for } 0 \leq \phi < 0.615 \text{ rad}, \\ \mathbf{1.0} & \text{for } 0.615 \text{ rad} < \phi \leq \pi/4. \end{cases} \quad (12)$$

These simple but important results for the zero-momentum band structure are displayed in Fig. 2. Each energy is given in units of $\epsilon_0 = \tau\beta c_0^2/(\hbar\omega)$, i.e., its actual value depends on the valley index τ , the ratio of the ellipse polarization axes β and the electron-light interaction strength. The “flat” band in fact no longer possesses this property, all three subbands are now distorted and intersect with each other. The energy band gap differs from $\lambda_0 c_0$ for graphene to $\lambda_0 c_0/2$ for a dice lattices. It is interesting to see that the band gap does not change for $\phi > 0.615 \text{ rad} \simeq 0.196\pi$ or $\alpha > 1/\sqrt{2}$. The band gap for a dice lattice is the smallest and is exactly half of that for graphene (the largest). The α -dependence of the band edge locations, presented in Fig. 2 (b) for comparison, is similar but not exactly identical with the corresponding dependence on ϕ .

An analytical solutions for finite- k energy dispersion could in principle be obtained, as it is always true for a third-power algebraic equation. However, the obtained expressions are quite lengthy and complicated so that they cannot be conveniently analyzed.

Our numerical results for the energy dispersions for the case of elliptically-polarized light are presented in Fig. 3. Leaving out the simplest case of $\phi = \pi/4$, which was discussed above and presented in Fig. 3 (a), we examine the remaining cases and see that the initially flat $\varepsilon_d(\mathbf{k}) = 0$ subband acquires a \mathbf{k} -dependent non-zero curvature and may be located either above or below the $\varepsilon = 0$ level depending on the phase as well as the valley index τ . The valence and conduction band edges are shifted in the vertical direction, so that there is no longer symmetry between the valence and conduction bands, as it was also pointed out in Ref. [2]. At the same time, there is complete inversion symmetry for $k_{\{x,y\}} \rightarrow -k_{\{x,y\}}$, which means that only even powers of the wave vector components k_x and k_y are present in the general eigenvalue equation based on the effective perturbation Hamiltonian (10). For all cases, the effect of the imposed irradiation on the flat band and its displacement from the zero-energy level are most noticeable at $\mathbf{k} = 0$. We emphasize that the anisotropy and the angular dependence in these dispersions appear only because of the anisotropy of the external perturbation field and is completely absent for the case of circularly-polarized irradiation with $\beta = 1$.

Not only the energy band gaps and edges from Eq. (12), but also the whole finite- k energy dispersion branches demonstrate direct and substantial dependence on the valley index $\tau = \pm 1$, as we see from Fig. 4. The location of each energy subband varies near the K and K' valleys, and this noticeable difference is not limited to a pure change of \pm sign, in contrast to all situations observed before. For $\alpha = 1/\sqrt{2}$, either upper or lower bandgap is closed,

depending on the value of τ . As a result, we obtain non-equivalent density of electronic states in each low-energy (K or K') region. The contributions from such electronic states from each valley is no longer equal or opposite to each other, which could strongly affect the transport properties.

These obtained dispersions show a striking resemblance to silicene, in which the electronic states with a given spin $\sigma = \pm 1$ demonstrate two inequivalent band gaps $\Delta_{\tau,\sigma} = |\Delta_{SO} - \sigma\tau\Delta_z|$, in which Δ_{SO} is a constant intrinsic spin-orbit gap and Δ_z can accept nearly any values depending on the external perpendicular electrostatic field. Consequently, varying the applied field, the gap between the bands can be opened or closed and a buckled honeycomb lattice appears to be in a topological insulator, valley-spin polarized metal (not gap) or a conventional band insulator state. The lower gap $|\Delta_{SO} - \Delta_z|$, which defines the actual band gap between the valence and conduction bands, becomes equal to the upper one $\Delta_{SO} + \Delta_z$, once either valley index τ or spin index σ is changed to its opposite value^{44,45}. This gives rise to specific transport properties⁴⁶ and a number of valleytronics applications,⁴⁷ which could now also be based on the irradiated α -T₃ lattice.

Finally, for graphene with $\varepsilon(|\mathbf{k}|) = \pm\hbar v_F|\mathbf{k}|$, interacting with circularly-polarized irradiation, the off-resonant dressed states have the following dispersion relations

$$\varepsilon_d^{\gamma=\pm 1}(\mathbf{k}) = \pm \left\{ \left(\frac{c_0^2}{\hbar\omega} \right)^2 + \left[\hbar v_F k \left\{ 1 - 2 \left(\frac{c_0}{\hbar\omega} \right)^2 \right\} \right]^2 \right\}^{1/2}, \quad (13)$$

which could be obtained as a limiting case of vanishing anisotropy for multi-layer black phosphorus,¹⁷ or setting to zero all the band gaps for transition metal dichalcogenides which were investigated in Ref. [16]. This result for graphene is a $\simeq 1/(\hbar\omega)^2$ approximation of well-known circularly-polarized irradiated quasiparticle dispersions. In contrast, an exact solution shows¹⁵ that the energy band gap is equal to

$$2\Delta_0(c_0|\omega) = \sqrt{(\hbar\omega)^2 + 4c_0^2} - \hbar\omega \simeq \frac{2c_0^2}{\hbar\omega} \cdot \left[1 - \left(\frac{c_0}{\hbar\omega} \right)^2 + \dots \right], \quad (14)$$

and the Fermi velocities in each direction are not affected. We again see that the field-induced energy bandgap for graphene is exactly twice as large when compared to a dice lattice.

B. Symmetric band structure and wave function for a dice lattice

Here, we address a specific case of spin-1 dice lattices without any dependence on α . This corresponds to $\phi = \pi/4$. Most importantly, all the equations are greatly simplified and additional closed-form analytical results could be obtained and investigated. Also it is crucial to see that the effect of irradiation is the lowest in this case for a given dressing field intensity, as we see from Figs. 3(c) and 3(d). This case has special significance for technical applications since those T-3 spin-1 materials could be possibly fabricated at the present time.

In this case, the non-interacting Hamiltonian (1) for a dice lattice takes the form

$$\mathbb{H}_\tau^d(\mathbf{k}) = \frac{\hbar v_F}{\sqrt{2}} \begin{bmatrix} 0 & k_\tau^- & 0 \\ k_\tau^+ & 0 & k_\tau^- \\ 0 & k_\tau^+ & 0 \end{bmatrix} = \sum_{\alpha=\pm} \hat{\Sigma}_\alpha^{(1)} k_\tau^\alpha, \quad (15)$$

where $\hat{\Sigma}_{\pm 1}^{(1)} = \hat{\Sigma}_x^{(1)} \pm i\hat{\Sigma}_y^{(1)}$ are defined based on spin-1 matrices in Appendix A.

The effective perturbation Hamiltonian (8) in this case up to the order of $1/(\hbar\omega)^2$ is

$$\hat{\mathcal{H}}_{\text{eff}}^{(E)}(\mathbf{k}, t) \simeq \begin{bmatrix} -\tau\beta/4 \cdot \lambda_0 c_0 & \mathcal{O}_\tau^{(-)}(\beta|\lambda_0, \mathbf{k}) & 0 \\ 0 & 0 & \mathcal{O}_\tau^{(-)}(\beta|\lambda_0, \mathbf{k}) \\ 0 & 0 & \tau\beta/4 \cdot \lambda_0 c_0 \end{bmatrix} + h.c., \quad (16)$$

where

$$\mathcal{O}_\tau^{(-)}(\beta|\lambda_0, \mathbf{k}) = \frac{\hbar v_F}{\sqrt{2}} \left[\tau k_x \left(1 + \beta^2 \frac{\lambda_0^2}{4} \right) - i k_y \left(1 + \frac{\lambda_0^2}{4} \right) \right]. \quad (17)$$

Such a dramatic simplification of Eq. (10) has been made possible mainly due to the fact that in our case $h_{12}(\beta | \tau, \phi) = h_{23}(\beta | \tau, \phi = \pi/4) = 1/\sqrt{2} \cdot (\beta^2 k_x - i\tau k_y)$.

For a Hamiltonian with such symmetry, the low-energy band structure is symmetric for electrons and holes with

$$\begin{aligned} \varepsilon_d^{(E)}(\beta | \lambda_0, \mathbf{k}) = 0 \quad \text{and} \quad \varepsilon_d^{(E)}(\beta | \lambda_0, \mathbf{k}) = \pm \sqrt{\mathcal{S}(\beta | \lambda_0, \mathbf{k})}, \quad \text{where} \\ \mathcal{S}(\beta | \lambda_0, \mathbf{k}) = \left(\frac{\beta}{4} \lambda_0 c_0 \right)^2 + (\hbar v_F)^2 \left\{ k^2 + \frac{\lambda_0^2}{2} \left[(\beta k_x)^2 \left(1 + \frac{\beta^2 \lambda_0^2}{8} \right) + k_y^2 \left(1 + \frac{\lambda_0^2}{8} \right) \right] \right\}. \end{aligned} \quad (18)$$

Only in this case, do the middle subbands remain flat for all wave vectors and the valence and conduction subbands stay completely symmetric for $\gamma = \pm 1$.

Equation (12) shows the opening of a finite energy band gap twice as large as $\Delta_0(\beta, \lambda_0) = \beta \lambda_0 c_0 / 2$. It is clear that the anisotropy of the energy bands is caused solely by the elliptical polarization of the dressing field and disappears for $\beta = 1$. From now on, we will focus only on the latter case of circularly-polarized irradiation. In this way, the energy label $\gamma = \pm 1$ still represents a Dirac cone with *renormalized isotropic* Fermi velocity $v_F^{(r)}(\lambda_0) = v_F \{ 1 + \lambda_0^2 / 2 (1 + \lambda_0^2 / 8) \}$.

We introduce the following simplifying notation: $\delta(\lambda_0, k) = \Delta_0(\beta = 1, \lambda_0) / [\hbar v_F^{(r)}(\lambda_0) k]$. This quantity is dimensionless, and it represents the induced energy gap related to a fixed electron energy for chosen non-zero wave vector k . For our case of small electron-light coupling with $\lambda_0 \ll 1$, it could be approximated by

$$\delta(\lambda_0 \ll 1, k) \simeq \frac{\lambda_0}{2} \frac{c_0}{\hbar v_F k} \left(1 - \frac{\lambda_0^2}{2} \right). \quad (19)$$

Now, we can obtain the wave functions, corresponding to dispersions in (18) as the eigenstates of the matrix (16). For the sake of simplicity, we will consider circularly-polarized light with $\beta = 1$. The solutions, pertaining to the valence and conduction bands $\gamma = \pm 1$ are

$$\Psi_d^{\gamma=\pm 1}(\tau | \lambda_0, \mathbf{k}) = \frac{1}{\sqrt{\mathcal{N}}} \begin{Bmatrix} \tau \mathcal{C}^{(1)} e^{-i\tau\theta_{\mathbf{k}}} \\ \mathcal{C}^{(2)} \\ \tau e^{+i\tau\theta_{\mathbf{k}}} \end{Bmatrix}. \quad (20)$$

where the component amplitudes and normalization factor may be obtained. In our case of low intensity of the incident radiation $c_0 \ll \hbar\omega$ these expressions could be simplified as

$$\begin{aligned} \mathcal{C}^{(1)}(\gamma | \lambda_0 \ll 1, k) &\simeq 1 + 2\delta(\lambda_0, k) [\gamma + \delta(\lambda_0, k)], \\ \mathcal{C}^{(2)}(\gamma | \lambda_0 \ll 1, k) &\simeq \sqrt{2} [\gamma - \delta(\lambda_0, k)] + \frac{\gamma}{\sqrt{2}} \delta^2(\lambda_0, k), \\ \mathcal{N}(\gamma | \lambda_0 \ll 1, k) &\simeq 4 [1 + 3\delta^2(\lambda_0, k)]. \end{aligned} \quad (21)$$

The components of the wave function (A10) are no longer equal to each other (apart from a common phase difference), as it is expected to occur when an energy gap is opened. Comparable alteration of the wave function components was demonstrated for irradiated graphene.³⁰ These components now also depend on the electron-hole index $\gamma = \pm 1$, i.e., their deflection from their initial $1/\sqrt{2}$ value is not the same for electrons and holes.

The remaining wave function for the flat band ($\gamma = 0$) is

$$\Psi_d^{\gamma=0}(\tau | \lambda_0, k) = \frac{1}{\sqrt{2[1 + \delta^2(\lambda_0, k)]}} \begin{Bmatrix} e^{-i\tau\theta_{\mathbf{k}}} \\ \sqrt{2}\delta(\lambda_0, k) \\ -e^{+i\tau\theta_{\mathbf{k}}} \end{Bmatrix}. \quad (22)$$

Here, one of its components is also inequivalent to the two others. This field-induced modification of the middle component and the normalization of the wave function (22) does not depend on the valley index τ .

C. Linear polarization of the incoming radiation

We now turn our attention to an alternative situation in which linearly-polarized radiation is incorporated into the α - T_3 model Hamiltonian. Being essentially anisotropic, such fields are known to transform the Dirac cone into an asymmetric elliptical cone without creating a gap between the valence and conduction bands.³⁴ Whereas in initially anisotropic phosphorene, the direction of the linear polarization was important,¹⁷ for the isotropic energy dispersions in $\alpha - T_3$ we can assume that the polarization vector lies along the x axis without any loss of generality so that

$$\mathbf{A}^{(L)}(t) = \left\{ \begin{array}{c} A_x^{(L)}(t) \\ 0 \end{array} \right\} = \frac{\mathcal{E}_0}{\omega} \left\{ \begin{array}{c} \cos(\omega t) \\ 0 \end{array} \right\}. \quad (23)$$

In each case of linear k-dependence, the total Hamiltonian of an interacting quasiparticle only acquires an additional term given by

$$\mathbb{H}_\tau^\phi(\mathbf{k}) \implies \hat{\mathcal{H}}^{(L)}(\mathbf{k}, t) = \mathbb{H}_\tau^\phi(\mathbf{k}) + \hat{\mathbb{H}}_A^{(L)}, \quad (24)$$

where

$$\hat{\mathbb{H}}_A^{(L)} = -\tau c_0 \cos(\omega t) \begin{bmatrix} 0 & \cos \phi & 0 \\ \cos \phi & 0 & \sin \phi \\ 0 & \sin \phi & 0 \end{bmatrix}. \quad (25)$$

The coupling constant $c_0 = v_F e E_0 / \omega$ is equivalent to that in the case of elliptically- or circularly-polarized light. We also note that each element of the matrix in (25) has identical periodic time dependence, which was not true for circularly-polarized irradiation field.

The case of linearly-polarized dressing field is distinguished because the time-dependent Schrödinger equation at K (or K') point for $\mathbf{k} = 0$ *could be solved exactly*. This means that our result regarding the absence of an energy bandgap is precise and, most crucially, a wave function with appropriate time dependence could be obtained in contrast to the previous case of elliptically polarized light.

The detailed derivation of the energy dispersions and the wave function for the linearly-polarized dressing field is provided in Appendix B. The dressed state quasiparticle energy dispersions are given by

$$\begin{aligned} \varepsilon_d^{(L)}(\phi | \lambda_0, \mathbf{k}) &= 0 \quad \text{and} \\ \varepsilon_d^{(L)}(\phi | \lambda_0, \mathbf{k}) &= \pm \hbar v_F \sqrt{\mathbb{A}(\theta_{\mathbf{k}} | \phi, \lambda_0)} k, \end{aligned} \quad (26)$$

with angular dependence

$$\mathbb{A}(\theta_{\mathbf{k}} | \phi, \lambda_0) = \cos^2 \theta + \left\{ [\mathcal{J}_0(2\lambda_0) \cos(2\phi)]^2 + [\mathcal{J}_0(\lambda_0) \sin(2\phi)]^2 \right\} \sin^2 \theta \quad (27)$$

clearly indicates *field-induced anisotropy*. The corresponding dispersion relations for graphene, obtained in Ref. [34], are immediately recovered if ϕ or α is set equal to zero. In the opposite limit for a *dice lattice* $\phi = \pi/4$, only the second term $\mathcal{J}_0(\lambda_0) \sin(2\phi)$ in Eq. (27) remains finite, so that the effect of electron-field interaction is the lowest.

Since our consideration is executed for off-resonant radiation with $\lambda_0 = c_0 / (\hbar\omega) \ll 1$, the zero-order Bessel function of the first kind could also be expanded so that the conduction and valence bands ($\gamma = \pm 1$) energy dispersions are further approximated as

$$\varepsilon_d^{(L)}(\phi | \lambda_0, \mathbf{k}) \simeq \pm \hbar v_F k \left\{ 1 - \frac{\lambda_0^2}{8} [5 + 3 \cos(4\phi)] \sin^2 \theta_{\mathbf{k}} \right\}. \quad (28)$$

Even for an infinitesimal coupling constant λ_0 , the anisotropy and, therefore, the difference between Fermi velocities in the k_x - and k_y -directions is the largest for graphene and the smallest in the dice lattice case.

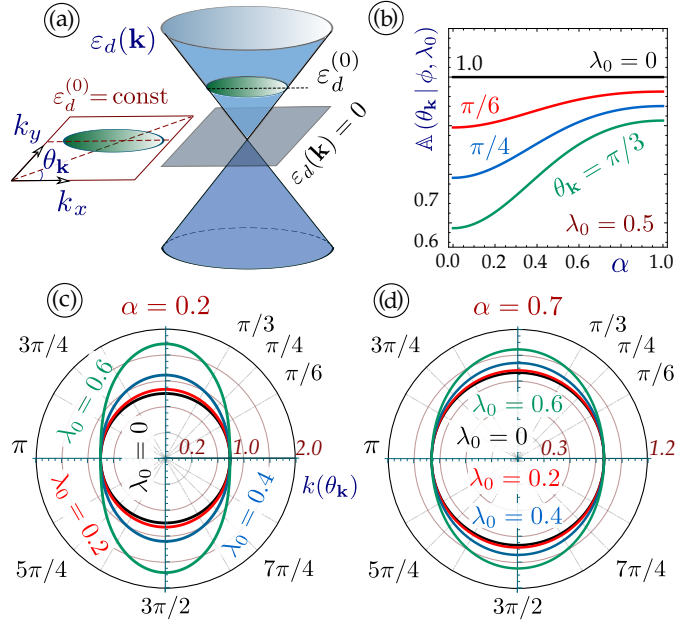


FIG. 5: (Color online) Angular dependence of dressed-state energy dispersions $\varepsilon_d^{(L)}(k, \theta_{\mathbf{k}})$, $\theta_{\mathbf{k}} = \tan^{-1}(k_y/k_x)$ for the case of linearly-polarized irradiation applied to an α - T_3 lattice, as it is schematically shown in panel (a). Plot (b) represents how the angular factor $\mathbb{A}(\theta_{\mathbf{k}} | \phi, \lambda_0)$, given by Eq. (27), depends on lattice parameter α at various angles $\theta_{\mathbf{k}}$ ($\theta_{\mathbf{k}} = \pi/6$ corresponds to a red line, $\pi/4$ - blue curve and $\theta_{\mathbf{k}} = \pi/3$ is depicted by the green line). The two lower polar plots (c) and (d) show the angular dependence of the obtained anisotropic dispersions (26) for chosen energy $\varepsilon_0 = 0.5 E_F$. In each plot, the curves are related to the different coupling parameters λ , as labeled. Here, $\lambda = 0$ is used for the black lines, $\lambda = 0.2$ for the red curves, $\lambda = 0.2$ for blue ones and $\lambda = 0.6$ for the green lines.

First and most important, we see that the flat band $\varepsilon(\mathbf{k}) = 0$ is not affected and remains dispersionless under linearly-polarized irradiation for all wave vectors. The valence and conduction bands become anisotropic, so that the standard right-circular Dirac cone is transformed into an elliptic cone with its major axis located along the direction of the light polarization. We also notice that the complete electron-hole symmetry of the upper and lower cones is preserved and there is no energy gap between the valence and conduction bands. These features are completely similar to the corresponding results for graphene.³⁴ However, an important novelty comes from the ϕ -dependence of the obtained dispersions. As we demonstrate in Fig. 4, the strength of induced anisotropy is related to the specific value of chosen ϕ .

Even though the procedure of deriving the corresponding wave functions, explained in Appendix B, is straightforward, the calculations are lengthy and tedious even for the simplest case of a dice lattice. The two wave functions, corresponding to the valence and conduction band energies with $\gamma = \pm 1$ are as follows

$$\begin{aligned} \Psi_d^{\gamma=\pm 1}(\lambda_0, \mathbf{k}) = \exp[\mp i v_F k t f_\theta] \frac{f_\theta + \cos \theta_{\mathbf{k}}}{4 f_\theta} \times \left[e^{\pm i z_\lambda(t)} \begin{Bmatrix} \tau \\ \pm \sqrt{2} \\ \tau \end{Bmatrix} - \right. \\ \left. - 2i \frac{\mathcal{J}_0(\lambda_0) \sin \theta_{\mathbf{k}}}{f_\theta + \cos \theta_{\mathbf{k}}} \begin{Bmatrix} 1 \\ 0 \\ -1 \end{Bmatrix} - \left[\frac{\mathcal{J}_0(\lambda_0) \sin \theta_{\mathbf{k}}}{f_\theta + \cos \theta_{\mathbf{k}}} \right]^2 \begin{Bmatrix} \tau \\ \mp \sqrt{2} \\ \tau \end{Bmatrix} e^{\mp i z_\lambda(t)} \right], \end{aligned} \quad (29)$$

where

$$f_\theta = \sqrt{\mathbb{A}(\theta_{\mathbf{k}} | \phi = \pi/4, \lambda_0)} = \left\{ \cos^2 \theta + [\sin \theta \mathcal{J}_0(\lambda_0)]^2 \right\}^{1/2} \quad (30)$$

and $z_\lambda(t) = \lambda_0 \sin(\omega t)$. Once its components are directly calculated, the wave function (29) takes the following form

$$\Psi_d^{\gamma=\pm 1}(\lambda_0, \mathbf{k}) = \frac{1}{2} \begin{Bmatrix} \tau e^{-i\Phi_\theta(\lambda_0)} \\ \gamma \sqrt{2} \\ \tau e^{i\Phi_\theta(\lambda_0)} \end{Bmatrix}, \quad (31)$$

$$\Phi_\theta(\lambda_0) = 2 \arctan \left[\tau \frac{\mathcal{J}_0(\lambda_0) \sin \theta_{\mathbf{k}}}{f_\theta + \cos \theta_{\mathbf{k}}} \right] \simeq \tau \left[\theta_{\mathbf{k}} - \frac{\lambda_0^2}{8} \sin^2(2\theta_{\mathbf{k}}) + \dots \right].$$

The components of this wave function are apparently equal to each other up to a phase difference similar to the non-interacting dice lattice wave functions, which corresponds to Eq. (2) and (2) for $\phi = \pi/4$. The phase difference $\Phi_\theta(\lambda_0)$ for a dice lattice is no longer equal to $\theta_{\mathbf{k}}$ and depends on the imposed irradiation intensity.

The remaining wave function for the flat band with $\gamma = 0$ is given by

$$\Psi_d^0(\lambda_0, \mathbf{k}) = \frac{1}{\sqrt{2} f_\theta} \times \left[-\frac{i\tau}{2} \sin \theta_{\mathbf{k}} \mathcal{J}_0(\lambda_0) \sum_{\alpha=\pm 1} e^{i\alpha z_\lambda(t)} \begin{Bmatrix} 1 \\ \alpha \sqrt{2} \tau \\ 1 \end{Bmatrix} + \cos \theta_{\mathbf{k}} \begin{Bmatrix} 1 \\ 0 \\ -1 \end{Bmatrix} \right]. \quad (32)$$

The structure of the obtained wave function in Eq. (32) is such that it again consists of two non-zero components of equal amplitude and phase difference $\Phi_\theta(\lambda_0)$. Consequently, we can rewrite the wave function (32) as

$$\Psi_d^0(\lambda_0, \mathbf{k}) = \frac{1}{\sqrt{2}} \begin{Bmatrix} e^{-i\Phi_\theta(\lambda_0)} \\ 0 \\ -e^{i\Phi_\theta(\lambda_0)} \end{Bmatrix}, \quad (33)$$

$$\Phi_\theta(\lambda_0) = \arctan [\tau \mathcal{J}_0(\lambda_0) \tan \theta_{\mathbf{k}}] \simeq \tau \left[\theta_{\mathbf{k}} - \frac{\lambda^2}{2} \sin(2\theta_{\mathbf{k}}) + \dots \right].$$

It is interesting to compare our results with the corresponding wave function for graphene obtained in Ref. [34]. The Dirac electron in graphene, interacting with a linearly-polarized off-resonant dressing field has the following dispersions

$$\begin{aligned} \varepsilon_d^{\gamma=\pm 1} &= \gamma \hbar v_F k \times f_\theta, \\ f_\theta &= \left\{ \cos^2 \theta_{\mathbf{k}} + [\mathcal{J}_0(2\lambda_0) \sin \theta_{\mathbf{k}}]^2 \right\}^{1/2}. \end{aligned} \quad (34)$$

The anisotropy factor f_θ for graphene is equivalent to our expression (B23) for ϕ or $\alpha = 0$. This is an opposite limit for the angular dependence in Eq. (B23) from the dice lattice with $\phi = \pi/4$, given in Eq. (B26).

The corresponding wave function at $t = 0$ could be rewritten as

$$\begin{aligned} \Psi_d^{\gamma=\pm 1}(\mathbf{k}) &= \frac{1}{\sqrt{2}} \begin{Bmatrix} 1 \\ \gamma \exp[i\Phi_\theta(\lambda_0)] \end{Bmatrix}, \\ \Phi_\theta(\lambda_0) &= 2 \arctan \left[\frac{\sin \theta_{\mathbf{k}} \mathcal{J}_0(\lambda_0)}{\cos \theta_{\mathbf{k}} + f_\theta} \right] \simeq \theta_{\mathbf{k}} - \frac{\lambda_0^2}{2} \sin(2\theta_{\mathbf{k}}) + \dots \end{aligned} \quad (35)$$

As it is expected for a distorted anisotropic Dirac cone, its wave function (35) has equal components, while their phase difference $\Phi_\theta(\lambda_0)$ depends on the interaction coefficient λ_0 .

For the general case of an α -T₃ lattice, the wave function is obtained as

$$\begin{aligned} \Psi_d^{\gamma=\pm 1}(\lambda_0, \mathbf{k}) &= \frac{1}{[\mathcal{N}_{23}^{(\phi)}]^{1/2}} \times \exp \left[\mp i v_F k t f_\theta^{(\phi)} \right] \times \\ &\times \left[\frac{r_1^{(\phi)}}{\sqrt{2}} \begin{Bmatrix} \tau \cos \phi \\ \pm 1 \\ \tau \sin \phi \end{Bmatrix} e^{\pm i z_\lambda(t)} + r_2^{(\phi)} \begin{Bmatrix} \sin \phi \\ 0 \\ -\cos \phi \end{Bmatrix} + \frac{r_3^{(\phi)}}{\sqrt{2}} \begin{Bmatrix} \tau \cos \phi \\ \mp 1 \\ \tau \sin \phi \end{Bmatrix} e^{\mp i z_\lambda(t)} \right], \end{aligned} \quad (36)$$

where the coefficients $r_{1,2}^{(\phi)}$ and the normalization function are defined in the Appendix B.

For the flat band with $\gamma = 0$, the wave function takes the form

$$\Psi_d^0(\lambda_0, \mathbf{k}) = \frac{1}{\sqrt{2\mathcal{N}_\theta^{(\phi)}}} \times \left[r_1^{(\phi)} \frac{\tau}{\sqrt{2}} \sum_{\alpha=\pm 1} e^{i\alpha z_\lambda(t)} \begin{Bmatrix} \cos \phi \\ \alpha \tau \\ \sin \phi \end{Bmatrix} + r_2^{(\phi)} \begin{Bmatrix} \sin \phi \\ 0 \\ -\cos \phi \end{Bmatrix} \right], \quad (37)$$

where

$$\begin{aligned} r_1^{(\phi)}(\lambda_0, \mathbf{k}) &= -i \sin(2\phi) \sin \theta_{\mathbf{k}} \mathcal{J}_0(\lambda_0), \\ r_2^{(\phi)}(\lambda_0, \mathbf{k}) &= \sqrt{2} [\cos \theta_{\mathbf{k}} + i\tau \cos(2\phi) \sin \theta_{\mathbf{k}} \mathcal{J}_0(2\lambda_0)]. \end{aligned} \quad (38)$$

The components of the wave function (37) are not equal to each other since this condition does not hold true even in the absence of irradiation, while all the previously obtained wave functions have components which differ only by a phase factor. This becomes explicit once the components of this wave function are evaluated

$$\Psi_d^0(\lambda_0, \mathbf{k}) = \frac{1}{\sqrt{\mathcal{N}_\theta^{(\phi)}}} \left\{ \begin{array}{c} \sin \phi \left[\cos \theta_{\mathbf{k}} - i\tau \sin \theta_{\mathbf{k}} \mathbb{X}_\theta^{(\phi)}(\lambda_0) \right] \\ 0 \\ -\cos \phi \left[\cos \theta_{\mathbf{k}} + i\tau \sin \theta_{\mathbf{k}} \left(2\mathcal{J}_0(\lambda_0) - \mathbb{X}_\theta^{(\phi)}(\lambda_0) \right) \right] \end{array} \right\}, \quad (39)$$

where, in our situation with $\lambda_0 \ll 1$, we can write

$$\begin{aligned} \mathbb{X}_\theta^{(\phi)}(\lambda_0) &\simeq 1 - \frac{\lambda_0^2}{4} [4 - 3 \cos(2\phi)], \\ 2\mathcal{J}_0(\lambda_0) - \mathbb{X}_\theta^{(\phi)}(\lambda_0) &\simeq 1 - \frac{\lambda_0^2}{4} [4 + 3 \cos(2\phi)], \\ \mathcal{N}_\theta^{(\phi)} &\simeq 1 - \frac{\lambda_0^2}{8} \{ 5 - [5 \cos(2\theta_{\mathbf{k}}) - 6 \cos(4\phi) \sin^2 \theta_{\mathbf{k}}] \}. \end{aligned} \quad (40)$$

The components of this wave function are not equal to each other, in contrast to all previously considered cases involving linearly-polarized field. The way they are modified in the presence of electron-photon interaction is not correlated with their initial values. Surprisingly, the normalization factors for all the obtained wave functions (29)-(32) and (36)-(37) do not depend on time.

III. BERRY PHASE MODIFICATION DUE TO THE DRESSING FIELD

As an evident and natural application for our novel photon-dressed electronic states obtained in Sec. II, we consider how the Berry phase of an α -T₃ or dice lattice is affected by the presence of an off-resonance dressing field with different polarizations. Specifically, we are interested in examining the way in which such quantum phases depend on α in the presence of finite electron-light coupling $\lambda_0 > 0$.

The Berry phase is defined as a geometrical phase difference, which a purely quantum system receives over a complete cycle of adiabatic, or isoenergetic evolution.⁴⁸⁻⁵⁰ All physically meaningful parameters, except for a quantum phase, are expected to return to their initial values over such a loop-like transformation. The Berry phase is logically connected to the quantal phase of *Aharonov and Bohm effect* for a charged particle moving along a closed path, which partially includes electrostatic or magnetic fields. Such topological phases strongly affect transport properties and lead to a finite conductivity at the band crossing even if the density of propagating waves at this point vanishes.⁵¹

As the first step, we are going to carry out a detailed investigation of the time-independent eigenstates, corresponding to the distorted Dirac cone due to an electron interacting with a dressing field. This could lead to either the opening of a band gap in the case of an elliptically- or circularly-polarized field, or an anisotropy of the dispersion relations due to a field with linear polarization. While in the former case the energy dispersions (18) were obtained using an effective perturbation Hamiltonian (8) without taking its actual time dependence into account, the wave functions

for the latter case involving linearly-polarized light were obtained with complete t -dependence, and therefore, need to be further clarified.

This could be viewed as a simplified model with an additional $\hat{\Sigma}_z$ term in graphene under circularly-polarized light¹⁷, which leads to considerable explanation of the considered phenomena, yet bears nearly all the crucial properties of irradiated graphene.³⁴ We will suppress the time dependence in Eqs. (36) and (37) and use their expressions at $t = 0$ for all further considerations. This will allow us to address a wider class of field-induced electronic states, not necessarily equivalent to dressed states under conditions discussed above.

In general, the time dependence of the obtained eigenstates, such as Eqs. (36) and (37), is expressed in exponential dependence of some of their components $\exp[\pm i z_\lambda(t)] = \exp[\pm i \lambda_0 \sin(\omega t)]$. In our consideration for an off-resonant field with $\lambda_0 \ll 1$, this dependence would lead to noticeable modification of the wave function components. Surprisingly, the normalization factors $\mathcal{N}_\theta^{(\phi)}$ for all types of α -T₃ materials under linearly-polarized irradiation, including the dice lattice limit, do not directly depend on time. Another occasion of direct time dependence is the initial phase factor $\exp[\mp i v_F k t f_\theta^{(\phi)}]$ in Eqs. (36) and (29), which does not affect most of its properties but leads to a linear increase of its Berry phase over time as $\sim v_F t f_\theta^{(\phi)}$.

The described situation of the time dependence is strikingly similar to the *electrostatic Aharonov-Bohm interference* effect.⁵² The wave function of a conventional Schrödinger particle of energy \mathbb{E} acquired a phase factor $\exp[i\phi]$, $\phi = -\mathbb{E}t/\hbar$. If such a particle is confined in the region with a constant electrostatic potential $V_0 = \text{constant}$, and zero electrostatic field, this potential affects the phase of the eigenstate as $\phi(t) - \phi(t = 0) = -eV_0 t/\hbar$. This additional phase affects the actual properties of the particle, as well as the outcome of a double-slit interference experiment, in spite of the fact that the actual electrostatic field is not present.

We can write the Berry phase as^{49,50}

$$\phi_B(\tau) = -i \oint_{\mathbb{C}} d\mathbf{k} \cdot \left\{ \left[\Psi_{\tau, \phi}^\gamma(\mathbf{k}) \right]^\dagger \vec{\nabla}_{\mathbf{k}} \Psi_{\tau, \phi}^\gamma(\mathbf{k}) \right\}, \quad (41)$$

where \mathbb{C} is a closed path within the 2D plane. For the case of non-irradiated wave functions of an α -T₃ lattice presented in Eqs. (2) and (3), the result is immediately obtained as $\phi_{\gamma=\pm 1, \tau}^B = \tau\pi \cos(2\phi)$ for the conduction and valence bands, and $\phi_{0, \tau}^B = 2\tau\pi \cos(2\phi)$ for the flat band at the K and K' valleys. These results *do not depend* on the choice of a closed curve \mathbb{C} , which in general cannot be true since the wave function components are k -dependent. We also remark that the Berry phase is gauge invariant and its value is unique up to $2\pi \times \text{integer}$.

The details on how to evaluate linear integral in Eq. (41) in polar coordinates in k -space for various types of incoming light polarization are provided in Appendix C. In our first case of circularly-polarized light, components (20) of the wave function (A9) are only k -dependent except for $\mathbf{e}^{\pm i\theta\mathbf{k}}$ factors, which are similar to those in the non-irradiated eigenstates (2) and (3), and the path of such isoenergetic linear integration is a circle of radius $k^{(0)}$. As a result, the Berry phase in the case of a dice lattice irradiated by a circularly-polarized dressing field is given by the following closed-form analytical expression

$$\phi_B^{(C)}(\tau = 1) = \frac{\{\mathcal{C}^{(1)}[k^{(0)}]\}^2 - 1}{\mathcal{N}^{(e)}[k^{(0)}]} \int_0^{2\pi} d\theta_{\mathbf{k}} \simeq \pi \frac{c_0}{\hbar v_F k^{(0)}} \lambda_0 \left[\gamma + \frac{c_0}{\hbar v_F k^{(0)}} \lambda_0 \right]. \quad (42)$$

The obtained Berry phases are not symmetric and are opposite for the electron and hole states except for the first-order term in the λ_0 expansion, as we also see from Fig. 6(a), even though this expression is exactly symmetric over the valley index $\tau = \pm 1$, i.e., $\phi_B^{(C)}(\tau = -1) = -\phi_B^{(C)}(\tau = 1)$, which is in complete analogy with the dice lattice in the absence of irradiation.⁵⁰ In summary, even for a dice lattice that does not have a finite Berry phase ($\phi_B^{(0)}(\tau) \sim \cos(2\phi) = 0$), it can be generated by a gap-opening elliptically- or circularly-polarized dressing field due to the variation of wave function components. While the dispersions are symmetric for a dice lattice, the wave function components, and therefore, the Berry phases do not share this property. The corresponding phase for the flat band is immediately obtained as zero, irrespective of the valley index or intensity of the incoming radiation since only the middle component in the eigenstate (22) is affected by the electron-light interaction, gives no contribution to Eq. (41).

Finally, we have calculated numerically the Berry phase for the α -T₃ lattice with an arbitrary ϕ in the presence of linearly-polarized irradiation. Our results are presented in Fig. 6. Panels (c) and (e) represent the results for the flat band, and the three right plots (b), (d) and (f) for the conduction band with $\gamma = 1$. In both cases, the phase is

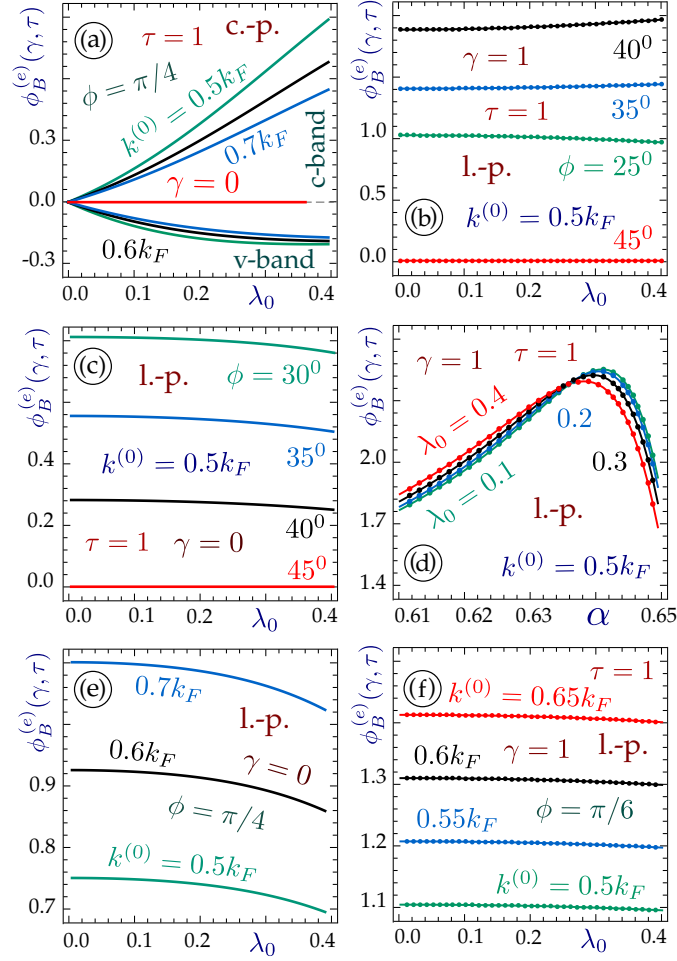


FIG. 6: (Color online) Berry phase for irradiated α - T_3 materials. Panel (a) corresponds to the circular polarization of the incident light, while all the others (b)-(f) are related to the linear type. Panel (a) shows the results for all bands, $\phi_B^{(e)} > 0$ for the conduction band, $\phi_B^{(e)} < 0$ for the valence band, and the values of Berry phase are not symmetric. However, it is always zero for the flat band. The remaining plots (c) and (e) on the left are related to the flat band of an α - T_3 lattice, and all the right panels (b), (d) and (f) to the conduction band with $\gamma = 1$. All plots except (d) show the Berry phase dependence on the coupling constant $\lambda_0 < 1$, but (d) shows a dependence on the parameter $\alpha = \tan \phi$ of an α - T_3 material. In panels (a) and (e), each black curve corresponds to $0.5 k_0$, the red curve to $0.6 k_0$ and the blue curve to $0.7 k_0$. Blue, black and red curves are related to $k^{(0)} = 0.55 k_0$, $0.6 k_0$ and $0.55 k_0$ in plot (f). Each line in panels (b) and (c) corresponds to a specific value of ϕ as labeled. In the case of a dice lattice with $\phi = \pi/4$, $\phi_B^{(e)} = 0$ disregarding the electron-light coupling.

zero for a dice lattice, disregarding the light intensity or the parameters of isoenergetic elliptic integral path so that the results in panel (d) are equal to zero in the limit $\alpha \rightarrow 1$, which confirms our previous analytical results obtained previously in Appendix C for a dice lattice under dressing field with linear polarization. The results for the flat band demonstrate a stronger dependence on the coupling constant, as well as on the parameters for an elliptic path of the linear integration. As we see from panel (d) of Fig. 6, the dependence of the Berry phase on λ_0 is not monotonic throughout the considered values of α , namely, the order in which all the curves corresponding to different λ_0 are laid out changed to exactly opposite ones when each line begins, passes its maximum value and starts decreasing as a function of α . Such non-monotonic dependence has not been observed for the case of circularly-polarized irradiation.

IV. CONCLUDING REMARKS

In this paper, we have executed a thorough investigation into electron-photon dressed states in α - T_3 lattices for all possible polarizations (elliptical, circular and linear) of the impinging radiation. We have derived closed-form expressions and analytic approximations for the quasiparticle energy dispersions for all types of such optical states.

We have demonstrated that the phase ϕ or the hopping parameter α plays a crucial role and affects the low-energy band structure for each type of polarization of the incident light. The obtained dressed states demonstrate both similarity and strong distinction compared to those earlier obtained in graphene or buckled honeycomb lattices. As an example, elliptically-polarized irradiation is connected with opening a band gap in the energy dispersions of α -T₃, symmetry breaking between the valence and conduction bands. The parameter α has also been shown to strongly affect the radiation-induced anisotropy and the angular dependence of the dressed quasiparticle dispersions for the case of a linearly-polarized external field. Generally speaking, we find that the effect of electron-light coupling is strongest for $\alpha \rightarrow 0$ (graphene), and is the weakest for a dice lattice with $\alpha = 1$ for both types of incoming light polarization.

We have found that for an elliptically-polarized field applied to a material with $\alpha \neq 1$, its low-energy band structure, including the gaps, directly depends on the $\tau = \pm 1$ valley index. This gives rise to valleytronics applications, which now could also be developed based on the irradiated α -T₃ lattice and enables electrically controllable valley filtering as being crucial for such applications and technology.

In addition to calculating the energy dispersion relations, we have obtained analytically the corresponding wave function for electrons dressed by an external field of various polarization. For elliptically-polarized light, the components of the obtained eigenstates are not equal to each other and do not just vary by a phase factor, as we have in the absence of irradiation (2) and (3). These components directly depend on the wavevector k and on the band index γ , so that the modification of the eigenstates in the valence, conduction and flat bands is not the same. This is the first obtained wave function for a dice lattice with a finite energy band gap.

Unlike previously discussed circularly-polarized irradiation, the eigenvalue equation for the linear polarization of the incident field allows for an exact solution for \mathbf{k} , so that we can claim with complete precision that in this case there is no energy gap between the conduction and valence bands, the flat band permanently stays dispersionless at the zero-energy level and complete symmetry between the bands is conserved. The effect of linearly-polarized dressing leads to the anisotropy of the Dirac cone dispersions similar to graphene. However, now we are able to tune the anisotropy and angular dependence of the energy band structure by adjusting the parameter α . Apart from the band symmetry breaking in the irradiated α -T₃ model reported in Ref. [2], we reveal a number of other crucial symmetries of the obtained dressed states, which could be broken or persist depending on the type and intensity of the applied field and the value of α .

The corresponding wave functions are drastically different for the dice lattice with $\alpha = 1$ and all other possible α -T₃ materials. In the former case, the components of such a dressed state are equal and differ only by a phase factor, which similar to anisotropic Dirac fermions in few-layer black phosphorus³⁵ are expected to reveal non-head-on asymmetric Klein paradox. In contrast, the components of such a wave function for arbitrary $0 < \alpha < 1$ differ from each other, which brings in considerable modification of their tunneling and transport properties. For a number of evaluations, we consider time-independent wave functions corresponding to $t = 0$ in order to address a wider class of phenomena pertaining to light-induced distortions of Dirac cone dispersions for α -T₃ lattices.

We also investigated Berry phases of the obtained dressed electron eigenstates in connection with their unusual composition and symmetric properties. The Berry phase is a specific quantum characteristic of an electronic state, which is particularly sensitive to a particle's environment and adiabatic change of external fields or their potentials. Such phases could be sometimes acquired by a system under consideration even if all the other important parameters and quantum numbers remain unaltered.

Berry phases are directly related to the wave function it is attributed to, its components, and the phase difference between them. For instance, the phases corresponding to the valence and conduction bands for a gap opening elliptically- or circularly-polarized irradiation even for the simplest dice lattice are not symmetric of opposite to each other, unlike their energy dispersions. We uncovered these relations in all their complexity and demonstrated that the phase of the flat band is always zero. The same is true for the phases of a dice lattice eigenstates for all bands ($\gamma = \pm 1$ and $\gamma = 0$) in the presence of an external field with linear polarization. For all other values of $\alpha \neq \pi/4$, we observed their moderate dependence on electron-light coupling λ_0 , parameter α and on the closed integration path, as it is expected to be according to the Aharonov-Bohm effect. The modification of the Berry phases pertaining to specific coupled electron-light states affect some of their important properties and could considerably modify the results of double-slit interference observations.

By studying the band structure of such optical electron states, we developed a useful methodology for laser-induced engineering of energy bands and tuning their most significant characteristics of α -T₃ innovative materials. Our results are expected to have a profound effect on the fabrication of modern optical and electronic devices and photonic crystals.

Acknowledgments

D.H. would like to acknowledge the support from the Air Force Office of Scientific Research (AFOSR). D.H is also supported by the DoD Lab-University Collaborative Initiative (LUCI) program. G.G. would like to acknowledge the support from the Air Force Research Laboratory (AFRL) through Grant #12530960.

Appendix A: Electron-field dressed states for elliptically- and circularly- polarizations applied to a dice lattice ($\phi = \pi/4$) - derivation of Eqs. (18), (20) and (22)

For a dice lattice, the time-independent perturbation operator (9) is expressed

$$\hat{\mathbb{P}}_\tau = -\frac{\tau c_0}{2\sqrt{2}} \sum_{\alpha=\pm} (1 - \alpha\tau\beta) \hat{\Sigma}_\alpha \quad (\text{A1})$$

in terms of

$$\Sigma_+^{(1)} = \begin{pmatrix} 0 & & \\ 0 & \mathbb{I}_{2 \times 2} & \\ 0 & 0 & 0 \end{pmatrix} = \begin{pmatrix} 0 & 1 & 0 \\ 0 & 0 & 1 \\ 0 & 0 & 0 \end{pmatrix} \quad \text{and} \quad \Sigma_-^{(1)} = \begin{bmatrix} 0 & 0 & 0 \\ \mathbb{I}_{2 \times 2} & 0 & \\ 0 & 0 & 0 \end{bmatrix} = \begin{bmatrix} 0 & 0 & 0 \\ 1 & 0 & 0 \\ 0 & 1 & 0 \end{bmatrix}. \quad (\text{A2})$$

The operators $\hat{\Sigma}_\pm^{(1)}$ are built from the spin-1 matrices

$$\hat{\Sigma}_x^{(1)} = \frac{1}{\sqrt{2}} \begin{pmatrix} 0 & 1 & 0 \\ 1 & 0 & 1 \\ 0 & 1 & 0 \end{pmatrix} \quad \text{and} \quad \hat{\Sigma}_y^{(1)} = \frac{1}{\sqrt{2}} \begin{pmatrix} 0 & -i & 0 \\ i & 0 & -i \\ 0 & i & 0 \end{pmatrix}, \quad (\text{A3})$$

where $\hat{\Sigma}_\pm^{(1)} = \hat{\Sigma}_x^{(1)} \pm i\hat{\Sigma}_y^{(1)}$, similarly to the case of 2×2 Pauli matrices for spin 1/2 used for graphene. Similarly, the energy gap exists if a $\hat{\Sigma}_z^{(1)}$ matrix is present in the Hamiltonian. In our case, this matrix is expressed as

$$\hat{\Sigma}_z^{(1)} = \frac{1}{\sqrt{2}} \begin{pmatrix} 1 & 0 & 0 \\ 0 & 0 & 0 \\ 0 & 0 & -1 \end{pmatrix}. \quad (\text{A4})$$

Finally, the effective perturbation Hamiltonian (10) is modified in the following way

$$\hat{\mathcal{H}}_{\text{eff}}^{(E)}(\mathbf{k}, t) = \frac{\hbar v_F}{\sqrt{2}} \sum_{\alpha=\pm} (\tau k_x - \alpha i k_y) \Sigma_\alpha^{(1)} - \frac{\tau\beta}{2} \lambda_0 \hat{\Sigma}_z^{(1)} + \hbar v_F \frac{\tau}{4\sqrt{2}} \lambda_0^2 \sum_{\alpha=\pm} (\beta^2 \tau k_x - \alpha i k_y) \Sigma_\alpha^{(1)}. \quad (\text{A5})$$

Using Hamiltonian (A5), we arrive at eigenvalue equation

$$\left[\varepsilon_d^{(L)}(\mathbf{k}) \right]^3 - \left(\frac{\beta c_0 \lambda_0}{2} \right)^2 \varepsilon_d^{(L)}(\mathbf{k}) - (\hbar v_F)^2 \left\{ \left[1 + \left(\frac{\beta \lambda_0}{2} \right)^2 \right]^2 k_x^2 + \left[1 + \left(\frac{\lambda_0}{2} \right)^2 \right]^2 k_y^2 \right\} \varepsilon_d^{(L)}(\mathbf{k}) = 0. \quad (\text{A6})$$

We see that the dispersions demonstrate complete e-h symmetry and renormalized Fermi velocity. Even though the exact evaluation of the wave function is not possible even for $\mathbf{k} = 0$ due to the complicated time dependence.

This way, the energy two $\gamma = \pm 1$ dispersions still represent a Dirac cone with *renormalized isotropic* Fermi velocity

$$v_F^{(r)}(\lambda_0) = v_F \left\{ 1 + \lambda_0^2/2 (1 + \lambda_0^2/8) \right\} \quad (\text{A7})$$

$$\delta(\lambda_0, \mathbf{k}) = \frac{\Delta_0(\beta = 1, \lambda_0)}{\hbar v_F^{(r)}(\lambda_0) k}. \quad (\text{A8})$$

This quantity is dimensionless, and it represents the induced energy gap related to a fixed electron energy for a given wave vector k .

Now we can obtain the wave functions, corresponding to dispersions (18) as the eigenstates of matrix (16). For the sake of simplicity, we will consider circularly-polarized light with $\beta = 1$. The solutions, pertaining to the valence and conduction bands $\gamma = \pm 1$ are

$$\Psi_d^{\gamma=\pm 1}(\tau | \lambda_0, k) = \frac{1}{\sqrt{\mathcal{N}^{(12)}}} \begin{Bmatrix} \tau \mathcal{C}^{(1)} e^{-i\tau\theta_{\mathbf{k}}} \\ \mathcal{C}^{(2)} \\ \tau e^{+i\tau\theta_{\mathbf{k}}} \end{Bmatrix}, \quad (\text{A9})$$

where $\mathcal{C}^{(1)}(\tau | \lambda_0, k)$, $\mathcal{C}^{(2)}(\tau | \lambda_0, k)$ and normalization factor $\mathcal{N}^{(12)}(\tau | \lambda_0, k)$ are

$$\mathcal{C}^{(1)}(\gamma | \lambda_0, k) = 1 + 2\delta^2(\lambda_0, k) + 2\gamma\delta(\lambda_0, k)\sqrt{1 + \delta^2(\lambda_0, k)}, \quad (\text{A10})$$

$$\mathcal{C}^{(2)}(\gamma | \lambda_0, k) = \sqrt{2}\gamma \left[\sqrt{1 + \delta^2(\lambda_0, k)} - \gamma\delta(\lambda_0, k) \right],$$

$$\mathcal{N}^{(12)}(\gamma | \lambda_0, k) = 1 + 2 \left[\sqrt{1 + \delta^2(\lambda_0, k)} - \gamma\delta(\lambda_0, k) \right]^2 + \left\{ 1 + 2\delta(\lambda_0, k) \left[\delta(\lambda_0, k) + \gamma\sqrt{1 + \delta^2(\lambda_0, k)} \right] \right\}^2.$$

For the flat band with $\gamma = 0$, the correlative eigenstate is given as

$$\Psi_d^{\gamma=0}(\tau | \lambda_0, \mathbf{k}) = \frac{1}{\sqrt{2[1 + \delta^2(\lambda_0, \mathbf{k})]}} \begin{Bmatrix} e^{-i\tau\theta_{\mathbf{k}}} \\ \sqrt{2}\delta(\lambda_0, k) \\ -e^{+i\tau\theta_{\mathbf{k}}} \end{Bmatrix}. \quad (\text{A11})$$

One can easily verify that the obtained wave functions (A9) and (A11) in the limit of vanishing electron-light interaction $\lambda_0 \rightarrow 0$ become equivalent to the dice lattice eigenstates, which are obtained from Eqs. (2) and (3) at $\phi = \pi/4$.

Appendix B: Linearly-polarized irradiation, derivation of Eqs. (27), (29)-(32) and (36)-(37).

The total Hamiltonian of a quasiparticle interacting with linearly-polarized field is

$$\hat{\mathcal{H}}(\mathbf{k}, t) = \hat{\mathbb{H}}_{\tau}^{\phi}(\mathbf{k}) + \hat{\mathbb{H}}_A^{(L)}. \quad (\text{B1})$$

It acquires an additional interaction term

$$\hat{\mathbb{H}}_A^{(L)} = -\tau c_0 \cos(\omega t) \begin{pmatrix} 0 & \cos \phi & 0 \\ \cos \phi & 0 & \sin \phi \\ 0 & \sin \phi & 0 \end{pmatrix}, \quad (\text{B2})$$

where the coupling amplitude $c_0 = v_F e E_0 / \omega$ is identical to that in the case of elliptically- or circularly-polarized light. So for $k_x = 0$ and $k_y = 0$ our equation is

$$i\hbar \frac{d\psi_0(t)}{dt} = \hat{\mathbb{H}}_A^{(L)} \psi_0(t). \quad (\text{B3})$$

The solutions of Eq. (B3) for the valence and conduction band edges with $\gamma = \pm 1$ are

$$\psi_0^{\tau, \gamma}(t) = \frac{1}{\sqrt{2}} \begin{Bmatrix} \tau \cos \phi \\ \gamma \\ \tau \sin \phi \end{Bmatrix} \exp [i\gamma \lambda_0 \sin(\omega t)] , \quad (\text{B4})$$

and for the flat band

$$\psi_0^{\gamma=0}(t) = \begin{Bmatrix} \sin \phi \\ 0 \\ -\cos \phi \end{Bmatrix} . \quad (\text{B5})$$

As it appears, the last wave function has no time dependence so each part of Eq. (B3) is equal to zero. These wave functions are clearly orthonormal and their structure demonstrates certain resemblance to the \mathbf{k} -dependent eigenfunctions (2) and (3) for the α - T_3 model.

The next step is to extend our solution to a finite wave vector. In order to achieve this, we need to solve the following time-dependent Schrödinger equation

$$i\hbar \frac{\partial}{\partial t} \Psi(\mathbf{k}, t) = \hat{\mathcal{H}}(\mathbf{k}, t) \Psi(\mathbf{k}, t) \quad (\text{B6})$$

for complete Hamiltonian (B1). At the K point, this expression becomes identical to Eq. (B3). We look for its solution in the form of the following expansion

$$\Psi(\mathbf{k}, t) = \sum_{\gamma=-1}^1 \mathcal{F}^{(\gamma)}(\mathbf{k}, t) \psi_0^\gamma(t) , \quad (\text{B7})$$

in which the unknown time- and k -dependent coefficients $\mathcal{F}^{(\gamma)}(\mathbf{k}, t)$ are to be found. Using Eq. (B3) for $\mathbf{k} = 0$ and the orthogonality of its solutions $\psi_0^\gamma(t)$, our initial system (B6) could be rewritten as

$$i\hbar \frac{\partial}{\partial t} \mathcal{F}^{(\gamma)}(\mathbf{k}, t) = \sum_{\rho=-1}^1 \mathcal{F}^{(\rho)} \langle \psi_0^\gamma(t) | \mathbb{H}_\tau^\phi(\mathbf{k}) | \psi_0^\rho(t) \rangle . \quad (\text{B8})$$

This leads to a set of three coupled linear partial differential equations

$$\frac{i}{v_F} \frac{\partial}{\partial t} \mathcal{F}^{(\mp 1)}(\mathbf{k}, t) = \mp k_x \mathcal{F}^{(\mp 1)} \mp \frac{i}{\sqrt{2}} e^{\pm i z_\lambda(t)} \sin(2\phi) k_y \mathcal{F}^{(0)} \mp i e^{\pm 2i z_\lambda(t)} \tau \cos(2\phi) k_y \mathcal{F}^{(\pm 1)} , \quad (\text{B9})$$

and

$$\frac{\partial}{\partial t} \mathcal{F}^{(0)}(\mathbf{k}, t) = \frac{v_F}{\sqrt{2}} \sin(2\phi) k_y \sum_{\alpha=\pm 1} \alpha e^{-i\alpha z_\lambda(t)} \mathcal{F}^{(-\alpha)} ,$$

where $z_\lambda(t) = \lambda_0 \sin \omega t$. Using Floquet theorem, we look for the dressed state quasiparticle energy dispersions $\varepsilon_d(\mathbf{k})$ by means of the following substitution^{2,17,34}

$$\mathcal{F}^{(\gamma)}(\mathbf{k}, t) = \exp \left\{ -\frac{i}{\hbar} \varepsilon_d(\mathbf{k}) t \right\} \sum_{n=-\infty}^{\infty} f_n^{(\gamma)} e^{in\omega t} . \quad (\text{B10})$$

The second term in expression (B10) is a periodic function of time (with the period $T_0 = 2\pi/\omega$), which is expanded in a Fourier series. Nested exponential function is traditionally reduced by the Jacobi-Anger series expansion

$$\exp \{ \pm \zeta \sin \omega t \} = \sum_{m=-\infty}^{\infty} \mathcal{J}_m(\pm \zeta) e^{im\omega t} , \quad (\text{B11})$$

where $\mathcal{J}_m(\zeta)$ is the Bessel function of the first kind. We also apply the orthogonality condition of the Fourier expansion function, namely,

$$\int_0^{2\pi/\omega} e^{i\omega n \cdot t} \cdot e^{-i\omega l \cdot t} dt = \delta_{n,l} = \begin{cases} 1 & \text{for } n = l, \\ 0 & \text{for } n \neq l \end{cases}$$

for any fixed number l ($-\infty < l < \infty$). By doing so, we arrive at the following system of coupled linear algebraic equations

$$\left[\mp k_x - \frac{\varepsilon_d(\mathbf{k})}{\hbar v_F} + l\omega \right] f_l^{(\mp 1)} \mp ik_y \sum_{m=-\infty}^{\infty} \left\{ \frac{1}{\sqrt{2}} \sin(2\phi) f_{l-m}^{(0)} \mathcal{J}_m(\pm\lambda_0) + \tau \cos(2\phi) f_{l-m}^{(\pm 1)} \mathcal{J}_m(\pm 2\lambda_0) \right\} = 0$$

and

$$\left[-\frac{\varepsilon_d(\mathbf{k})}{\hbar v_F} + l\omega \right] f_l^{(0)} + \frac{i}{\sqrt{2}} \sin(2\phi) k_y \sum_{m=-\infty}^{\infty} \sum_{\alpha=\pm 1} \alpha \mathcal{J}_m(-\alpha \lambda_0) f_{l-m}^{(-\alpha)} = 0. \quad (\text{B12})$$

Next, we follow the standard procedure^{17,34} of eliminating the terms $f_{l \neq 0}^{(\rho)} = 0$ ($\rho = -1, 0, 1$). The point here is that for the case of off-resonant interaction, which satisfies $\hbar\omega \gg \varepsilon_d(\mathbf{k})$ and $\omega \gg v_F k_{\{x,y\}}$, all the terms in the square brackets in each equation of system (B13) are negligible compared to $l\omega$ for any $l \neq 0$. The system is simplified to a new set of equations

$$f_l^{(\mp 1)} = \pm \frac{ik_y}{l\omega} \sum_{m=-\infty}^{\infty} \left\{ \frac{1}{\sqrt{2}} \sin(2\phi) f_{l-m}^{(0)} \mathcal{J}_m(\pm\lambda_0) + \tau \cos(2\phi) f_{l-m}^{(\pm 1)} \mathcal{J}_m(\pm 2\lambda_0) \right\}$$

and

$$f_l^{(0)} = -\frac{i}{\sqrt{2}l\omega} \sin(2\phi) k_y \sum_{m=-\infty}^{\infty} \sum_{\alpha=\pm 1} \alpha \mathcal{J}_m(-\alpha \lambda_0) f_{l-m}^{(-\alpha)}, \quad (\text{B13})$$

which can not be satisfied unless all the expansion coefficients $f_l^{(-1,0,1)} = 0$ for $l \neq 0$, at least due to the fact that in this case one specific coefficient $f_l^{(\rho)}$ which we are looking for must be much smaller than all the others. Once only $l = 0$ terms are left, our system (B13) is dramatically simplified and now becomes

$$\left[\overleftrightarrow{\mathcal{K}}_{\tau}(\mathbf{k} | \phi, \lambda_0 \ll 1) - \frac{\varepsilon_d(\mathbf{k})}{\hbar v_F} \right] \otimes \begin{Bmatrix} f_0^{(-1)} \\ f_0^{(0)} \\ f_0^{(1)} \end{Bmatrix} = 0, \quad (\text{B14})$$

where

$$\overleftrightarrow{\mathcal{K}}_{\tau}(\mathbf{k} | \phi, \lambda_0 \ll 1) = \begin{bmatrix} -k_x/2 & -i/\sqrt{2} \sin(2\phi) k_y \mathcal{J}_0(\lambda_0) & -i\tau \cos(2\phi) k_y \mathcal{J}_0(2\lambda_0) \\ 0 & 0 & -i/\sqrt{2} \sin(2\phi) k_y \mathcal{J}_0(\lambda_0) \\ 0 & 0 & k_x/2 \end{bmatrix} + h.c. \quad (\text{B15})$$

Here, *h.c.* means adding a Hermitian conjugate matrix, exactly as we had in Eq. (16), and we also used the fact that zero-order Bessel function is even, i.e., $\mathcal{J}_0(\xi) = \mathcal{J}_0(-\xi) \simeq 1 - \xi^2/4$, $\xi = \lambda_0$ and $2\lambda_0$.

As the final result of this derivation, we obtain the dressed state quasiparticle energy dispersions

$$\begin{aligned} \varepsilon_d(\mathbf{k}) &= 0 \quad \text{and} \\ \varepsilon_d(\mathbf{k}) &= \pm \hbar v_F \sqrt{\mathbb{A}(\theta_{\mathbf{k}} | \phi, \lambda_0)} k, \end{aligned} \quad (\text{B16})$$

which angular dependence

$$\mathbb{A}(\theta_{\mathbf{k}} | \phi, \lambda_0) = \cos^2 \theta + \left\{ [\mathcal{J}_0(2\lambda_0) \cos(2\phi)]^2 + [\mathcal{J}_0(\lambda_0) \sin(2\phi)]^2 \right\} \sin^2 \theta \quad (\text{B17})$$

clearly demonstrates the anisotropy of the energy dispersions induced by the electron-photon interaction. We immediately recover the corresponding result graphene³⁴ if ϕ is equal to zero. For a dice lattice with $\phi = \pi/4$, only second term $\mathcal{J}_0(\lambda_0) \sin(2\phi)$ remains non-zero and the effect of dressing field is the lowest.

In our case of off-resonant radiation with low intensity with $\lambda = c_0^{(L)}/(\hbar\omega) \ll 1$, the zero-order Bessel function of the first kind could be expanded as shown above, so that the conduction and valence bands energy dispersions are further approximated as

$$\varepsilon_d^{\gamma=\pm 1}(\mathbf{k}) \simeq \gamma \hbar v_F \left\{ k^2 - \frac{\lambda_0^2}{4} [5 + 3 \cos(4\phi)] k_y^2 \right\}^{1/2}. \quad (\text{B18})$$

The anisotropy and the difference between the Fermi velocities in the k_x and k_y directions in both valence and conduction bands is the largest for $\phi = 0$ and the smallest for a dice lattice case.

The corresponding wave function for the dressed state quasiparticle, obtained directly from Eq. (B7), is

$$\begin{aligned} \Psi_d^{\gamma=\pm 1}(\lambda_0, \mathbf{k}) &= \frac{1}{[\mathcal{N}_{23}^{(\phi)}]^{1/2}} \times \exp[\mp i v_F k t f_\theta^{(\phi)}] \times \\ &\times \left[\frac{r_1^{(\phi)}}{\sqrt{2}} \begin{Bmatrix} \tau \cos \phi \\ \pm 1 \\ \tau \sin \phi \end{Bmatrix} e^{\pm i z_\lambda(t)} + r_2^{(\phi)} \begin{Bmatrix} \sin \phi \\ 0 \\ -\cos \phi \end{Bmatrix} + \frac{r_3^{(\phi)}}{\sqrt{2}} \begin{Bmatrix} \tau \cos \phi \\ \mp 1 \\ \tau \sin \phi \end{Bmatrix} e^{\mp i z_\lambda(t)} \right], \end{aligned} \quad (\text{B19})$$

where

$$\begin{aligned} r_1^{(\phi)}(\lambda_0, \mathbf{k}) &= 2f_\theta^{(\phi)} \left(f_\theta^{(\phi)} + \cos \theta_{\mathbf{k}} \right) - \mathcal{J}_0^2(\lambda_0) \sin^2 \theta_{\mathbf{k}} \sin^2(2\phi), \\ r_2^{(\phi)}(\lambda_0, \mathbf{k}) &= -i\sqrt{2} \sin \theta_{\mathbf{k}} \sin(2\phi) \mathcal{J}_0(\lambda_0) \left[f_\theta^{(\phi)} + \cos \theta_{\mathbf{k}} + i\tau \sin \theta_{\mathbf{k}} \cos(2\phi) \mathcal{J}(2\lambda_0) \right], \\ r_3^{(\phi)}(\lambda_0, \mathbf{k}) &= -\sin \theta_{\mathbf{k}} \left[\sin \theta_{\mathbf{k}} \sin^2(2\phi) \mathcal{J}_0^2(\lambda_0) + 2i\tau f_\theta^{(\phi)} \cos(2\phi) \mathcal{J}_0(2\lambda_0) \right]. \end{aligned} \quad (\text{B20})$$

The normalization factor is done by evaluating each component of the wave function

$$\begin{aligned} \mathcal{N}_{23}^{(\phi)} &= \left| \frac{\tau \cos \phi}{\sqrt{2}} \left[r_1^{(\phi)}(\lambda_0, \mathbf{k}) + r_3^{(\phi)}(\lambda_0, \mathbf{k}) \right] + r_2^{(\phi)}(\lambda_0, \mathbf{k}) \sin \phi \right|^2 + \frac{1}{2} \left| r_1^{(\phi)}(\lambda_0, \mathbf{k}) - \right. \\ &\left. - r_3^{(\phi)}(\lambda_0, \mathbf{k}) \right|^2 + \left| \frac{\tau \sin \phi}{\sqrt{2}} \left[r_1^{(\phi)}(\lambda_0, \mathbf{k}) + r_3^{(\phi)}(\lambda_0, \mathbf{k}) \right] - r_2^{(\phi)}(\lambda_0, \mathbf{k}) \cos \phi \right|^2. \end{aligned} \quad (\text{B21})$$

For the flat band with $\gamma = 0$, the wave function takes the form

$$\Psi_d^0(\lambda_0, \mathbf{k}) = \frac{1}{\sqrt{2\mathcal{N}_\theta^{(\phi)}}} \times \left[r_1^{(\phi)} \frac{\tau}{\sqrt{2}} \sum_{\alpha=\pm 1} e^{i\alpha z_\lambda(t)} \begin{Bmatrix} \cos \phi \\ \alpha \tau \\ \sin \phi \end{Bmatrix} + r_2^{(\phi)} \begin{Bmatrix} \sin \phi \\ 0 \\ -\cos \phi \end{Bmatrix} \right], \quad (\text{B22})$$

where

$$\begin{aligned} r_1^{(\phi)}(\lambda_0, \mathbf{k}) &= -i \sin(2\phi) \sin \theta_{\mathbf{k}} \mathcal{J}_0(\lambda_0), \\ r_2^{(\phi)}(\lambda_0, \mathbf{k}) &= \sqrt{2} [\cos \theta_{\mathbf{k}} + i\tau \cos(2\phi) \sin \theta_{\mathbf{k}} \mathcal{J}_0(2\lambda_0)]. \end{aligned} \quad (\text{B23})$$

or, clearly presenting its component, we write

$$\begin{aligned}
\Psi_d^0(\lambda_0, \mathbf{k}) &= \frac{1}{\sqrt{\mathcal{N}_\theta^{(\phi)}}} \left\{ \begin{array}{c} \sin \phi \left[\cos \theta_{\mathbf{k}} - i\tau \sin \theta_{\mathbf{k}} \mathbb{X}_\theta^{(\phi)}(\lambda_0) \right] \\ 0 \\ -\cos \phi \left[\cos \theta_{\mathbf{k}} + i\tau \sin \theta_{\mathbf{k}} \left(2\mathcal{J}_0(\lambda_0) - \mathbb{X}_\theta^{(\phi)}(\lambda_0) \right) \right] \end{array} \right\}, \quad (\text{B24}) \\
\mathbb{X}_\theta^{(\phi)}(\lambda_0) &= 2 \cos^2 \phi \mathcal{J}_0(\lambda_0) - \cos(2\phi) \mathcal{J}_0(2\lambda_0) \simeq 1 - \frac{\lambda_0^2}{4} [4 - 3 \cos(2\phi)], \\
2\mathcal{J}_0(\lambda_0) - \mathbb{X}_\theta^{(\phi)}(\lambda_0) &\simeq 1 - \frac{\lambda_0^2}{4} [4 + 3 \cos(2\phi)], \\
\mathcal{N}_\theta^{(\phi)} &= \cos^2 \theta_{\mathbf{k}} + \sin^2 \theta_{\mathbf{k}} \left\{ \left[\mathbb{X}_\theta^{(\phi)}(\lambda_0) \right]^2 + (2 \cos \phi)^2 \mathcal{J}_0(\lambda_0) \left[\mathcal{J}_0(\lambda_0) - \mathbb{X}_\theta^{(\phi)}(\lambda_0) \right] \right\} \simeq \\
&\simeq 1 - \frac{\lambda_0^2}{8} \left\{ 5 - [5 \cos(2\theta_{\mathbf{k}}) - 6 \cos(4\phi) \sin^2 \theta_{\mathbf{k}}] \right\}.
\end{aligned}$$

1. Dice lattice, $\alpha = 1.0$

As a general rule, the results are greatly simplified for the case of a dice lattice

$$\begin{aligned}
\Psi_d^{\gamma=\pm 1}(\lambda_0, \mathbf{k}) &= \exp[\mp i v_F k t f_\theta] \frac{f_\theta + \cos \theta_{\mathbf{k}}}{4 f_\theta} \times \left[e^{\pm i z_\lambda(t)} \left\{ \begin{array}{c} \tau \\ \pm \sqrt{2} \\ \tau \end{array} \right\} - \right. \\
&\left. - 2i \frac{\mathcal{J}_0(\lambda_0) \sin \theta_{\mathbf{k}}}{f_\theta + \cos \theta_{\mathbf{k}}} \left\{ \begin{array}{c} 1 \\ 0 \\ -1 \end{array} \right\} - \left[\frac{\mathcal{J}_0(\lambda_0) \sin \theta_{\mathbf{k}}}{f_\theta + \cos \theta_{\mathbf{k}}} \right]^2 \left\{ \begin{array}{c} \tau \\ \mp \sqrt{2} \\ \tau \end{array} \right\} e^{\mp i z_\lambda(t)} \right], \quad (\text{B25})
\end{aligned}$$

where

$$f_\theta = \sqrt{\mathbb{A}(\theta_{\mathbf{k}} | \phi = \pi/4, \lambda_0)} = \left\{ \cos^2 \theta + [\sin \theta \mathcal{J}_0(\lambda_0)]^2 \right\}^{1/2} \quad (\text{B26})$$

and we once again use our previous notation $z_\lambda(t) = \lambda_0 \sin(\omega t)$. This wave function could be presented in a specifically simplified way

$$\begin{aligned}
\Psi_d^{\gamma=\pm 1}(\lambda_0, \mathbf{k}) &= \frac{1}{2} \left\{ \begin{array}{c} \tau e^{-i\Phi_\theta(\lambda_0)} \\ \gamma \sqrt{2} \\ \tau e^{i\Phi_\theta(\lambda_0)} \end{array} \right\}, \quad (\text{B27}) \\
\Phi_\theta(\lambda_0) &= 2 \arctan \left[\tau \frac{\mathcal{J}_0(\lambda_0) \sin \theta_{\mathbf{k}}}{f_\theta + \cos \theta_{\mathbf{k}}} \right] \simeq \tau \left[\theta_{\mathbf{k}} - \frac{\lambda_0^2}{8} \sin^2(2\theta_{\mathbf{k}}) + \dots \right].
\end{aligned}$$

Phase $\Phi_\theta(\lambda_0)$ for a dice lattices differs from that in graphene by the argument of the Bessel function and the expansion coefficient.

The remaining wave function for the flat band with $\gamma = 0$ takes the following form

$$\Psi_d^0(\lambda_0, \mathbf{k}) = \frac{1}{\sqrt{2} f_\theta} \times \left[-\frac{i\tau}{2} \sin \theta_{\mathbf{k}} \mathcal{J}_0(\lambda_0) \sum_{\alpha=\pm 1} e^{i\alpha z_\lambda(t)} \left\{ \begin{array}{c} 1 \\ \alpha \sqrt{2} \tau \\ 1 \end{array} \right\} + \cos \theta_{\mathbf{k}} \left\{ \begin{array}{c} 1 \\ 0 \\ -1 \end{array} \right\} \right]. \quad (\text{B28})$$

The structure of the obtained wave function (B28) is such that at $t = 0$ it consists of two components of equal amplitudes and phase difference $\Phi_\theta(\lambda_0)$, and could be rewritten as

$$\Psi_d^0(\lambda_0, \mathbf{k}) = \frac{1}{\sqrt{2}} \begin{Bmatrix} e^{-i\Phi_\theta(\lambda_0)} \\ 0 \\ -e^{i\Phi_\theta(\lambda_0)} \end{Bmatrix}, \quad (\text{B29})$$

$$\Phi_\theta(\lambda_0) = \arctan[\tau \mathcal{J}_0(\lambda_0) \tan \theta_{\mathbf{k}}] \simeq \tau \left[\theta_{\mathbf{k}} - \frac{\lambda_0^2}{2} \sin(2\theta_{\mathbf{k}}) + \dots \right].$$

It is straightforward to verify that in the limit of vanishing electron-photon interaction $\lambda_0 = c_0/(\hbar\omega) \implies 0$ all our obtained wave functions (B19)-(B22) and (B25)-(B28) are exactly equivalent to the α -T₃ lattice eigenstates (2) and (3) or to the corresponding dice lattice limit with $\phi = \pi/4$.

Appendix C: Dressing field-induced adjustments to Berry phases, derivation of Eq. (42) and theoretical background for our numerical results presented in Fig. 6.

In this appendix, we provide the details of the *Berry phase* evaluation for the obtained dresses states wave functions (20) and (22) for the case of circularly-polarized field applied to a dice lattice, as well as for eigenstates (29)-(32) and (36)-(37), corresponding to various types of α -T₃ lattices interacting with irradiation with linear polarization.

In polar coordinates, the general expression for gradient $\vec{\nabla}_k$ and the vector length element $d\mathbf{k}$ ⁵³

$$\begin{aligned} \vec{\nabla}_k &= \frac{\partial}{\partial k} \hat{e}_k + \frac{1}{k} \frac{\partial}{\partial \theta_{\mathbf{k}}} \hat{e}_\theta, \\ d\mathbf{k} &= dk \hat{e}_k + k d\theta_{\mathbf{k}} \hat{e}_\theta. \end{aligned} \quad (\text{C1})$$

As the first step, we must choose the right *closed integration path* for Eq. (41). In order to satisfy the requirement of an adiabatic, or isoenergetic evolution of a quantum system, during which a Berry phase is acquired, we have to choose a path with a constant energy of our quisparticle, i.e., with $\varepsilon_{\tau, \phi}^{\gamma=\pm 1}(\mathbf{k}) = \varepsilon_0 = \text{const}$.

For the first case of a circularly-polarized light, the energy dispersions (18) and the corresponding eigenstates (20) and (22) are isotropic, so that the required path ought to be a *circle of radius $k^{(0)}$* . While the wave function components and their scalar product can still depend on both k - and $\theta_{\mathbf{k}}$ -components of the two-dimensional vector \mathbf{k} , the integration variable in Eq. (41) is modified as $d\mathbf{k} = k^{(0)} d\theta_{\mathbf{k}} \hat{e}_\theta$.

We begin with the eigenstate (20) for the valence and conduction bands. In the simplest case of a circular path of radius $k^{(0)}$, the Berry phase defined in Eq. (41) is equal to

$$\phi_B^{(e)}(\tau = 1) = \frac{[\mathcal{C}^{(1)}(k^{(0)})]^2 - 1}{\mathcal{N}^{(e)}(k^{(0)})} \int_0^{2\pi} d\theta_{\mathbf{k}} \simeq \pi \gamma \frac{c_0}{\hbar v_F k^{(0)}} \lambda_0. \quad (\text{C2})$$

while in the vicinity of K' valley this result is exactly opposite $\phi_B^{(e)}(\tau = -1) = -\phi_B^{(e)}(\tau = 1)$, similarly to the case of non-irradiated α -T₃. In the absence of the irradiation, the Berry phase for a dice lattice is zero - $\phi_B^{(0)}(\tau) = \tau\pi \cos(\pi/2) = 0$.⁵⁰ The corresponding Berry phase for the flat band remains zero in the presence of circularly-polarized light, which could be confirmed by evaluating integral (41) for wave function (22).

In contrast, the constant-energy cut for dispersions (26) with angular dependence (27) has an elliptic shape, as it shown in Fig. 4 (a). Such an ellipse is described as

$$\left(\frac{k_x^{(e)}}{a} \right)^2 + \left[\frac{k_y^{(e)}}{b(\lambda_0, \phi)} \right]^2 = 1, \quad (\text{C3})$$

where

$$a = \frac{\varepsilon_0}{\hbar v_F}, \quad (\text{C4})$$

$$b(\lambda_0, \phi) = \frac{\varepsilon_0}{\hbar v_F} \left\{ [\mathcal{J}_0(2\lambda_0) \cos(2\phi)]^2 + [\mathcal{J}_0(\lambda_0) \sin(2\phi)]^2 \right\}^{-1} \simeq a \left\{ 1 + \frac{\lambda_0^2}{8} [5 + 3 \cos(4\phi)] \right\} > a.$$

Elliptical path in polar coordinates is given by

$$k^{(e)}(\theta_{\mathbf{k}}) = ab(\lambda_0, \phi) \left\{ (a \cos \theta_{\mathbf{k}})^2 + [b(\lambda_0, \phi) \sin \theta_{\mathbf{k}}]^2 \right\}^{-1/2} = \frac{b}{\sqrt{1 - [e(\lambda_0, \phi) \cos \theta_{\mathbf{k}}]^2}}, \quad (\text{C5})$$

where a and $b(\lambda_0, \phi)$ are major and minor semi-axes of an ellipse in the k -space and $e(\lambda_0) = \sqrt{1 - [b(\lambda_0, \phi)/a]^2}$ is its *eccentricity*. We see that each specific elliptical path and its eccentricity depends on the incoming radiation intensity or coupling constant λ_0 . Our notation $\theta_{\mathbf{k}} = \arctan(k_y/k_x)$ should not lead to a confusion since in the polar coordinates angle $\theta_{\mathbf{k}}$ is independent from the radial component k .

$$dk^{(e)}(\theta_{\mathbf{k}}) = -\frac{1}{2} b(\lambda_0, \phi) e(\lambda_0, \phi)^2 \frac{\sin(2\theta_{\mathbf{k}}) d\theta_{\mathbf{k}}}{[1 - e(\lambda_0, \phi)^2 \cos^2 \theta_{\mathbf{k}}]^{2/3}} \quad (\text{C6})$$

and

$$d\mathbf{k} = \frac{b(\lambda_0, \phi) d\theta_{\mathbf{k}}}{\sqrt{1 - e(\lambda_0, \phi)^2 \cos^2 \theta_{\mathbf{k}}}} \left\{ \hat{e}_\theta - \frac{e(\lambda_0, \phi)^2 \sin(2\theta_{\mathbf{k}})}{2 [1 - e(\lambda_0, \phi)^2 \cos^2 \theta_{\mathbf{k}}]} \hat{e}_k \right\}. \quad (\text{C7})$$

In the case of linearly-polarized dressing field, the wave function components depend only on angle $\theta_{\mathbf{k}}$ but not on the radial component k for all possible values of α .

For $\alpha = 1$, all the relevant \hat{e}_θ -components of the gradient all equal to zero. Indeed, for wave functions (31) or (33),

$$\vec{\nabla}_{\mathbf{k}} \Psi_{\tau, \phi}^\gamma(\mathbf{k}) = \frac{1}{k^{(e)}(\theta_{\mathbf{k}})} \frac{\partial}{\partial \theta_{\mathbf{k}}} \Psi_{\tau, \phi}^\gamma(\mathbf{k}) = \frac{i\tau}{2k^{(e)}(\theta_{\mathbf{k}})} e^{-i\Phi_\theta(\lambda_0)} \frac{\partial \Phi_\theta(\lambda_0)}{\partial \theta_{\mathbf{k}}} \begin{pmatrix} -1 \\ 0 \\ 1 \end{pmatrix} \quad (\text{C8})$$

so that $\left[\Psi_{\tau, \phi}^\gamma(\mathbf{k}) \right]^\dagger \vec{\nabla}_{\mathbf{k}} \Psi_{\tau, \phi}^\gamma(\mathbf{k}) = 0$.

The only difference between the valence/conduction and the flat bands here is the exact expression of $\Phi_\theta(\lambda_0)$, which does not play any crucial role. The middle component of each wave function does not contribute to Eq. (41) since its $\partial/\partial \theta_{\mathbf{k}}$ derivative is always zero.

-
- ¹ J. D. Malcolm and E. J. Nicol, Physical Review B **93**, 165433 (2016).
 - ² B. Dey and T. K. Ghosh, Physical Review B **98**, 075422 (2018).
 - ³ K. Novoselov, A. K. Geim, S. Morozov, D. Jiang, M. Katsnelson, I. Grigorieva, S. Dubonos, and A. Firsov, nature **438**, 197 (2005).
 - ⁴ R. R. Nair, P. Blake, A. N. Grigorenko, K. S. Novoselov, T. J. Booth, T. Stauber, N. M. Peres, and A. K. Geim, Science **320**, 1308 (2008).
 - ⁵ A. C. Ferrari, J. Meyer, V. Scardaci, C. Casiraghi, M. Lazzeri, F. Mauri, S. Piscanec, D. Jiang, K. Novoselov, S. Roth, et al., Physical review letters **97**, 187401 (2006).
 - ⁶ M. Rizzi, V. Cataudella, and R. Fazio, Physical Review B **73**, 144511 (2006).
 - ⁷ J. Vidal, R. Mosseri, and B. Douçot, Physical review letters **81**, 5888 (1998).
 - ⁸ N. Goldman and J. Dalibard, Physical review X **4**, 031027 (2014).
 - ⁹ P. Perez-Piskunow, G. Usaj, C. Balseiro, and L. F. Torres, Physical Review B **89**, 121401 (2014).
 - ¹⁰ E. S. Morell and L. E. F. Torres, Physical Review B **86**, 125449 (2012).
 - ¹¹ Z. Gu, H. Fertig, D. P. Arovas, and A. Auerbach, Physical review letters **107**, 216601 (2011).
 - ¹² V. Kozin, I. Iorsh, O. Kibis, and I. Shelykh, Physical Review B **97**, 035416 (2018).
 - ¹³ S. Mandal, T. Liew, and O. Kibis, Physical Review A **97**, 043860 (2018).
 - ¹⁴ S. Morina, O. V. Kibis, A. A. Pervishko, and I. A. Shelykh, Phys. Rev. B **91**, 155312 (2015).
 - ¹⁵ O. Kibis, Physical Review B **81**, 165433 (2010).
 - ¹⁶ O. Kibis, K. Dini, I. Iorsh, and I. Shelykh, Physical Review B **95**, 125401 (2017).
 - ¹⁷ A. Iurov, L. Zhemchuzhna, G. Gumbs, and D. Huang, Journal of Applied Physics **122**, 124301 (2017).
 - ¹⁸ O. Kibis, K. Dini, I. Iorsh, and I. Shelykh, Semiconductors **52**, 523 (2018).
 - ¹⁹ T. Oka and H. Aoki, Physical Review B **79**, 081406 (2009).

- ²⁰ B. Dóra, J. Cayssol, F. Simon, and R. Moessner, *Physical review letters* **108**, 056602 (2012).
- ²¹ D. Abergel and T. Chakraborty, *Applied Physics Letters* **95**, 062107 (2009).
- ²² H. L. Calvo, J. S. Luna, V. Dal Lago, and L. E. F. Torres, *Physical Review B* **98**, 035423 (2018).
- ²³ V. Dal Lago, E. S. Morell, and L. F. Torres, *Physical Review B* **96**, 235409 (2017).
- ²⁴ G. Usaj, P. Perez-Piskunow, L. F. Torres, and C. Balseiro, *Physical Review B* **90**, 115423 (2014).
- ²⁵ A. Iurov, G. Gumbs, O. Roslyak, and D. Huang, *Journal of Physics: Condensed Matter* **25**, 135502 (2013).
- ²⁶ D. Yudin, O. Kibis, and I. Shelykh, *New Journal of Physics* **18**, 103014 (2016).
- ²⁷ I. Iorsh, K. Dini, O. Kibis, and I. Shelykh, *Physical Review B* **96**, 155432 (2017).
- ²⁸ M. Katsnelson, K. Novoselov, and A. Geim, *Nature physics* **2**, 620 (2006).
- ²⁹ H. L. Calvo, H. M. Pastawski, S. Roche, and L. E. F. Torres, *Applied Physics Letters* **98**, 232103 (2011).
- ³⁰ A. Iurov, G. Gumbs, O. Roslyak, and D. Huang, *Journal of Physics: Condensed Matter* **24**, 015303 (2011).
- ³¹ G. Gumbs, A. Iurov, D. Huang, P. Fekete, and L. Zhemchuzhna, in *AIP Conference Proceedings* (AIP, 2014), vol. 1590, pp. 134–142.
- ³² S. Morina, K. Dini, I. V. Iorsh, and I. A. Shelykh, *ACS Photonics* **5**, 1171 (2018).
- ³³ A. Iurov, G. Gumbs, and D. Huang, *Journal of Modern Optics* **64**, 913 (2017).
- ³⁴ K. Kristinsson, O. Kibis, S. Morina, and I. Shelykh, *Scientific reports* **6**, 20082 (2016).
- ³⁵ Z. Li, T. Cao, M. Wu, and S. G. Louie, *Nano letters* **17**, 2280 (2017).
- ³⁶ E. Illes and E. Nicol, *Physical Review B* **95**, 235432 (2017).
- ³⁷ D. F. Urban, D. Bercioux, M. Wimmer, and W. Häusler, *Physical Review B* **84**, 115136 (2011).
- ³⁸ E. Illes, J. Carbotte, and E. Nicol, *Physical Review B* **92**, 245410 (2015).
- ³⁹ A. Raoux, M. Morigi, J.-N. Fuchs, F. Piéchon, and G. Montambaux, *Physical review letters* **112**, 026402 (2014).
- ⁴⁰ F. Piéchon, J. Fuchs, A. Raoux, and G. Montambaux, in *Journal of Physics: Conference Series* (IOP Publishing, 2015), vol. 603, p. 012001.
- ⁴¹ E. Illes and E. Nicol, *Physical Review B* **94**, 125435 (2016).
- ⁴² T. Biswas and T. K. Ghosh, *Journal of Physics: Condensed Matter* **28**, 495302 (2016).
- ⁴³ T. Biswas and T. K. Ghosh, *Journal of Physics: Condensed Matter* **30**, 075301 (2018).
- ⁴⁴ C. J. Tabert and E. J. Nicol, *Physical Review B* **89**, 195410 (2014).
- ⁴⁵ M. Ezawa, *New Journal of Physics* **14**, 033003 (2012).
- ⁴⁶ A. Iurov, G. Gumbs, and D. Huang, *Physical Review B* **98**, 075414 (2018).
- ⁴⁷ H.-Y. Xu, L. Huang, D. Huang, and Y.-C. Lai, *Physical Review B* **96**, 045412 (2017).
- ⁴⁸ M. V. Berry, *Proc. R. Soc. Lond. A* **392**, 45 (1984).
- ⁴⁹ D. Xiao, M.-C. Chang, and Q. Niu, *Reviews of modern physics* **82**, 1959 (2010).
- ⁵⁰ E. Illes, Ph.D. thesis (2017), URL <http://atrium.lib.uoguelph.ca/xmlui/handle/10214/11512>.
- ⁵¹ T. Louvet, P. Delpace, A. A. Fedorenko, and D. Carpentier, *Physical Review B* **92**, 155116 (2015).
- ⁵² Y. Aharonov and D. Bohm, *Physical Review* **115**, 485 (1959).
- ⁵³ G. B. Arfken and H. J. Weber, *Mathematical methods for physicists* (1999).